



Universidad  
Carlos III de Madrid

Trabajo Fin de Grado

---

**EXPERIMENTAL STUDY OF  
THE STEADY STREAMING  
AROUND CYLINDERS**

---

by

**Eduardo Merino Gonzalez**

**June 2015**

---

Under the supervision of:

dr. W. Coenen

*Departamento de Ingenieria Termica y de Fluidos*

*Universidad Carlos III de Madrid*

### **Acknowledgement**

To my tutor Wilfried Coenen, for giving me the chance to experience how real scientists work and think.

This project is also thanks to my classmates during these four years, for creating the atmosphere that has helped us to improve every day.

And specially to my family, for showing me the value of giving the most of myself.

## Abstract

The purpose of this project is the study of the *steady streaming* phenomenon induced by different distributions of circular cylinders oscillating within a fluid.

To understand whether this characteristic flow would be suitable for trapping micro-particles, the influence of the main parameters governing this phenomenon was analysed, varying them within two different geometrical distributions. In the first one, placing two cylinders symmetrically, to extend and contrast the previous results for this case. And in the second set of experiments, a distribution of four cylinders forming a square was used instead, to analyse its outcome as it was unexplored so far.

In order to achieve these objectives, several experiments were performed during this research. To recreate the conditions needed, the laboratory set-up was formed by a tank full of water and glass particles that reflect the light, a laser beam to create a visual plane, and the structure containing the cylinders. Meanwhile, a high-speed camera is in charge of capturing the position of the particles at every given period of time.

After gathering all the raw data, the images were processed by several Matlab codes which are able to extract the important information about the movement of the particles and display the tendency they are following. Then, the outcome was compared and contrasted with previous experiments and numerical studies to confirm its validity and understand its meaning.

Through this analysis, it is concluded that the experiments achieved during this project can confirm the previous hypothesis and ratify former studies. Moreover, it has been possible to provide a wider overview of the importance of the parameters that govern the *steady streaming* and extend the knowledge about potential uses for new distributions of circular cylinders.

# Contents

|           |                                   |    |
|-----------|-----------------------------------|----|
| 1         | Introduction . . . . .            | 7  |
| 1.1       | The phenomenon . . . . .          | 7  |
| 1.2       | State of art . . . . .            | 12 |
| 1.1.2.a   | Technological Challenge . . . . . | 12 |
| 1.1.2.b   | Previous studies . . . . .        | 14 |
| 1.3       | Objectives . . . . .              | 20 |
| 1.4       | Project plan . . . . .            | 21 |
| 2         | Formulation . . . . .             | 23 |
| 2.1       | Geometry . . . . .                | 23 |
| 2.2.1.a   | Two cylinders . . . . .           | 23 |
| 2.2.1.b   | Four cylinders . . . . .          | 24 |
| 2.2.1.b.1 | Distribution 1 . . . . .          | 24 |
| 2.2.1.b.2 | Distribution 2 . . . . .          | 24 |
| 2.2       | The movement . . . . .            | 26 |
| 2.3       | Dimensionless analysis . . . . .  | 27 |
| 3         | Experimental procedure . . . . .  | 31 |
| 3.1       | Procedure . . . . .               | 31 |
| 3.2       | The setup . . . . .               | 33 |
| 3.3.2.a   | Tank and support system . . . . . | 33 |
| 3.3.2.b   | Laser . . . . .                   | 34 |
| 3.3.2.c   | Motor . . . . .                   | 36 |
| 3.3.2.d   | Cylinders . . . . .               | 37 |
| 3.3.2.e   | Movement transmission . . . . .   | 38 |
| 3.3.2.f   | Electronic control . . . . .      | 39 |
| 3.3.2.g   | Camera and software . . . . .     | 40 |
| 3.3       | Image processing . . . . .        | 42 |
| 4         | Results . . . . .                 | 47 |

---

|                     |   |           |
|---------------------|---|-----------|
| 4.1                 | Experiments with two cylinders . . . . .  | 47        |
| 4.2                 | Experiments with four cylinders . . . . . | 56        |
| 5                   | Conclusions . . . . .                     | 63        |
| 5.1                 | Two cylinders . . . . .                   | 63        |
| 5.2                 | Four cylinders . . . . .                  | 67        |
| <b>Bibliography</b> |   | <b>71</b> |

# List of Figures

|    |  |    |
|----|--|----|
| 1  | Steady Streaming around one cylinder. An <i>et al.</i> (2011) . . . . .  | 7  |
| 2  | Instant Streaming movement at the wall of one cylinder . . . . .   | 8  |
| 3  | Steady streaming vortices for one cylinder. Sadhal (2012) . . . . .  | 9  |
| 4  | Distribution for two cylinders . . . . .   | 10 |
| 5  | Steady Streaming over two cylinders . . . . .  | 11 |
| 6  | Trapping techniques . . . . .  | 13 |
| 7  | Acoustic particle trapping. Ding <i>et al.</i> (2012) . . . . .  | 14 |
| 8  | Steady Streaming streamlines over a sphere by Riley (1966) . . . . .   | 15 |
| 9  | Steady Streaming experiment between a cylinder and a wall by<br>Wybrow, Yan and Riley (1996) . . . . .                                       | 16 |
| 10 | Time averaged streamlines of the Navier-Stokes solution by Wybrow<br>et al (1996) . . . . .  | 16 |
| 11 | Schematic of the inner hearing system of a fish. Kotas <i>et al.</i> (2007)  | 17 |
| 12 | Steady streaming around a vertically oscillated sphere at $R_M =$<br>84, $\varepsilon = 0.1$ and $a = 1.27cm$ . Kotas et al (2007) . . . . . | 18 |
| 13 | Flow distribution for $\phi = \frac{\pi}{2}$ . $\varepsilon \ll 1$ and $R_s \gg 1$ . Coenen and<br>Riley (2009) . . . . .                    | 18 |
| 14 | Experimental flow distribution by Galan (2013) . . . . .   | 19 |
| 15 | Geometry for experiments using two cylinders . . . . .   | 24 |
| 16 | Geometry for experiments using four cylinders. Distribution 1 . . . . .  | 25 |
| 17 | Geometry for experiments using four cylinders. Distribution 2 . . . . .  | 25 |
| 18 | Definition of the real variables . . . . .   | 27 |
| 19 | Scheme of the laboratory set-up . . . . .  | 31 |
| 20 | Water tank and support system . . . . .  | 33 |
| 21 | Laser . . . . .  | 34 |
| 22 | Laser emitting . . . . .   | 35 |
| 23 | Laser plane regions . . . . .  | 35 |

|    |  |    |
|----|--|----|
| 24 | Laser plane regions with the mirrors . . . . .   | 35 |
| 25 | Electric Motor . . . . .   | 36 |
| 26 | Voltage generator . . . . .  | 36 |
| 27 | Distribution for two cylinders . . . . .   | 37 |
| 28 | Distribution for four cylinders . . . . .  | 37 |
| 29 | Oscillation movement transmission . . . . .  | 39 |
| 30 | Electronic circuit . . . . .   | 40 |
| 31 | Camera set-up . . . . .  | 41 |
| 32 | Camera . . . . .   | 41 |
| 33 | Visual noise contained in the raw images . . . . .   | 43 |
| 34 | Clean processed image . . . . .  | 43 |
| 35 | Identification of the cylinders . . . . .  | 44 |
| 36 | Streamlines during steady streaming . . . . .  | 45 |
| 37 | Set of experiments Type A . . . . .  | 48 |
| 38 | Stationary period at $t_1$ . Experiment for $Rs = 155.16$ $\varepsilon = 0.14$ . .         | 49 |
| 39 | Stationary period at $t_2$ . Experiment for $Rs = 155.16$ $\varepsilon = 0.14$ . .         | 49 |
| 40 | Stationary period at $t_3$ . Experiment for $Rs = 155.16$ $\varepsilon = 0.14$ . .         | 50 |
| 41 | Stationary period at $t_4$ . Experiment for $Rs = 155.16$ $\varepsilon = 0.14$ . .         | 50 |
| 42 | Real geometry parameters for experiments type A . . . . .                                  | 51 |
| 43 | Parameters for experiment type A . . . . .   | 51 |
| 44 | Streamlines distribution. Experiment A1: $\varepsilon = 0.14$ y $Rs = 71.76$               | 52 |
| 45 | Streamlines distribution. Experiment A2: $\varepsilon = 0.14$ y $Rs = 97.94$               | 53 |
| 46 | Streamlines distribution. Experiment A3: $\varepsilon = 0.14$ y $Rs = 144.49$              | 54 |
| 47 | Streamlines distribution. Experiment A4: $\varepsilon = 0.14$ y $Rs = 195.89$              | 55 |
| 48 | Real geometry parameters for experiments B and C . . . . .                                 | 56 |
| 49 | Parameters for experiments B and C . . . . .   | 57 |
| 50 | Streamlines distribution. Experiment B1: $\varepsilon = 0.14$ y $Rs =$<br>168.74 . . . . . | 58 |
| 51 | Streamlines distribution. Experiment B2: $\varepsilon = 0.14$ y $Rs =$<br>168.74 . . . . . | 59 |
| 52 | Streamlines distribution. Experiment C1: $\varepsilon = 0.14$ y $Rs = 73.70$               | 60 |
| 53 | Streamlines distribution. Experiment C2: $\varepsilon = 0.14$ y $Rs =$<br>167.77 . . . . . | 61 |
| 54 | Detail of Experiment A4: $\varepsilon = 0.14$ y $Rs = 195.89$ . . . . .                    | 64 |
| 55 | Diagram of steady streaming over two cylinders . . . . .                                   | 64 |
| 56 | Detail of the streamlines for experiment A1. $\varepsilon = 0.14$ y $Rs = 71.76$           | 65 |
| 57 | Detail of the streamlines for experiment A2. $\varepsilon = 0.14$ y $Rs = 97.94$           | 66 |

|    |   |    |
|----|---|----|
| 58 | Detail of the streamlines for experiment A3. $\varepsilon = 0.14$ y $Rs = 144.49$ | 67 |
| 59 | Detail of the streamlines for experiment B1. $\varepsilon = 0.14$ y $Rs = 168.74$ | 68 |
| 60 | Detail of the streamlines for experiment C1. $\varepsilon = 0.14$ y $Rs = 73.70$  | 69 |



# • INTRODUCTION •

# 1 Introduction

## 1.1 The phenomenon

Steady streaming is a nonzero time-averaged flow motion experienced by a fluid when is influenced by the action of nonlinear Reynolds stresses near no-slip boundaries of a solid. In the case of this project, this solid body will be a circular cylinder where, as a result of this interaction, some characteristic flow patterns are induced in the fluid. As it can be seen in the simplification of the Figure 1, from An *et al.* (2011), four small recirculating cells appear attached to the walls of the cylinder, as well as several bigger ones with their centres further away from them.

Paying attention to the direction of the movement of the fluid around the cylinder, it can be also appreciated the existence of two ejection points at the top and bottom ends of the body. Meanwhile, the fluid is pulled to the right and left sides, creating these expected vortices.

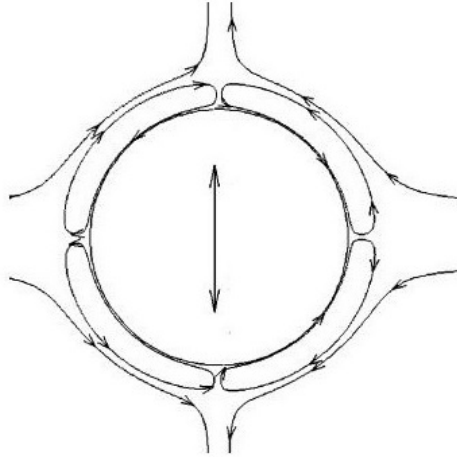


Figure 1: Steady Streaming around one cylinder. An *et al.* (2011)

However, this just represents the net movement that the fluid describes caused by this phenomenon. In fact, if the steady streaming is analysed in smaller periods of time, it can be noticed that the particles keep swinging up and down all the way while they describe a bigger movement trajectory, as in

Figure 2.

This displacement makes sense attending to the oscillation of the cylinder, which pushes and pulls the fluid in opposite directions every cycle. It is also interesting that this continuous sway of the particles along the walls is slow, despite the bodies usually oscillates with bigger velocities.

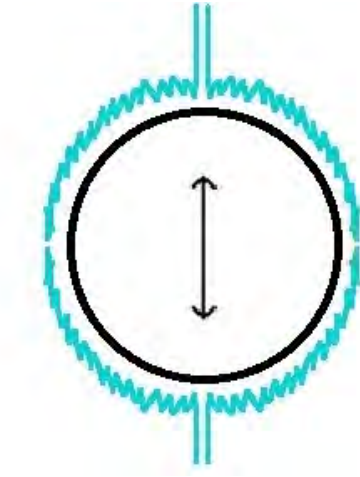


Figure 2: Instant Streaming movement at the wall of one cylinder

As it will be studied in detail in further sections of the project, dimensional analysis can be applied to steady streaming created by an oscillating flow around a circular object to identify the variables governing the phenomenon.

Through this method, it will be concluded that the parameters to watch are:

- Nondimensional oscillation amplitude

$$\varepsilon = \frac{A}{r}$$

Where  $A$  is the movement amplitude and  $r$  is the object radius

- Streaming Reynolds number

$$Rs = \varepsilon Re = \frac{\varepsilon \omega r^2}{\nu}$$

Where  $\omega$  is the angular oscillation frequency and  $\nu$  the kinematic viscosity

Actually, one of the aims of this investigation is to explore the results of using  $Rs \gg 1$  and  $\varepsilon \ll 1$ . The case with high streaming Reynolds number and low oscillation amplitude hasn't been deeply analysed yet by former studies but there are clues that evidence the potential interest of this case.

When  $\varepsilon$  is small enough, at leading order the flow is basically inviscid with viscous effects at thin Stokes layers at the surface of the body. However, if it is too big, flow separation becomes a problem and in some cases of circular cylinders Honji vortices may also appear in the longitudinal plane. Therefore, when trying to create microeddies for particle trapping a value of  $\varepsilon \ll 0.25$  is recommended.

Regarding to this streaming Reynolds number, if  $Rs \ll 1$ , the streaming flow is mainly Stokes flow, meaning the velocities are too weak. As the regime get close to  $Rs \sim 1$ , the particle trapping is viable and 4 microeddies in the case of a cylinder, arise around the body (Figure 3). However, it is not until  $Rs \gg 1$  that the eddies become stronger making the trapping forces big enough for many other applications.

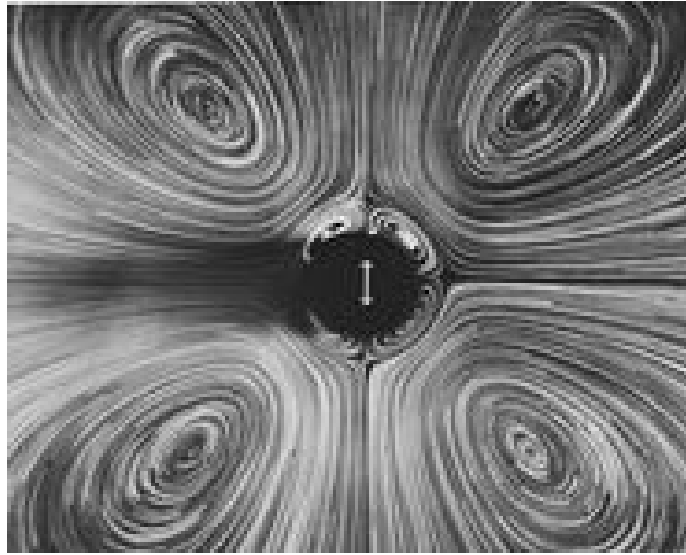


Figure 3: Steady streaming vortices for one cylinder. Sadhal (2012)

Moreover, these patterns turn more interesting when several solid bodies are placed close enough to influence the same region of the fluid simultaneously. The ejection points are affected between them and new flow structures appear around the cylinders. This project has especially focused on this interaction between single steady streaming phenomena created by different cylinders.

The experiments about what happens when two cylinders oscillate at the same time while they are close enough have led to some interesting conclusions. Former studies using this laboratory set-up used a distribution like in figure 4, placing the cylinders separated by a distance  $D = 2r$  and making them move with streaming Reynolds number bigger than one.

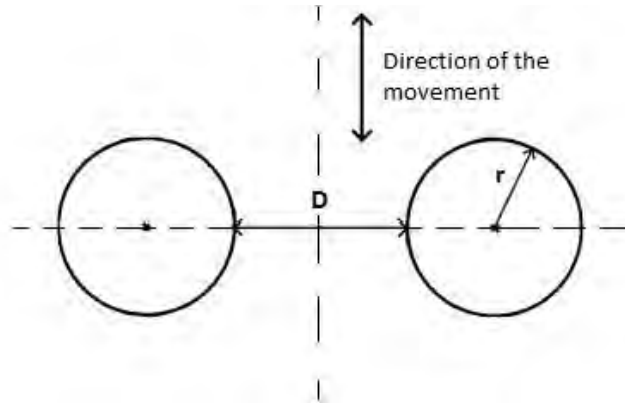


Figure 4: Distribution for two cylinders

As a result, a modification in the recirculating cells was noticed, since now both jets emerging from the ejection points are influencing each other. As it can be seen in Figure 5, four major groups of vortices appear when this distribution is used. However, now the jets coming out from the ejection points  $E_1$  and  $E_2$  vary their trajectory and head towards each other. Meanwhile, the fluid contained between the cylinders is pulled by each of them generating two stagnation points  $SP_1$  and  $SP_2$ , as well as in either sides of the bodies  $S_1$  and  $S_2$ .

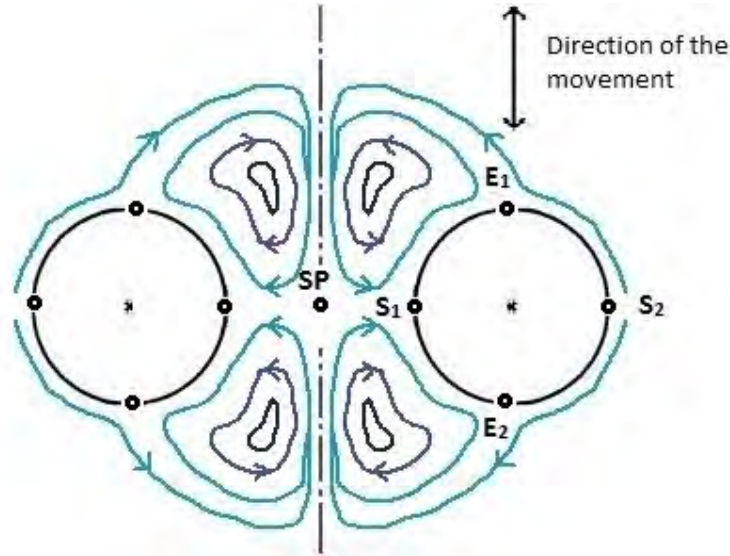


Figure 5: Steady Streaming over two cylinders

In the case of placing multiple cylinders, the experiments made show that the recirculating cells are heavily influenced by the ones nearby. Through the method of asymptotic expansions for two cylinders, the tutor of this project in collaboration with N. Riley found out that the velocity at the edge of the stokes layers is strongly modified due to the presence of the other moving body. This creates four microeddies per cylinder so 4 trapping positions can be used.

However, in the case of  $Rs \gg 1$ , these cells appear this time in the outer streaming flow. Moreover, making use of Particle Image Velocimetry (PIV) it can be checked that the speed associated to them for the same value of radius  $r$  and fluid viscosity  $\nu$  is one order of magnitude stronger.

## 1.2 State of art

### 1.1.2.a Technological Challenge

In the actual framework of the technological development, the ability to identify and control certain particles in a fixed position has turned into a decisive process for many interesting applications.

Plenty of them are found for instance in the field of the bioengineering, where being able to scan and capture microparticles and cells present in a fluid becomes the key for the progress in many detection processes. Traditionally, these objectives were aimed by using the *patch-clamp* technique, consisting in trying to micro-pipetting the single specimen desired. Nonetheless, this process is slow, laborious and very difficult to repeat automatically, making it unfeasible for most bio-applications.

However, the necessity of trapping these particles through a non-invasive method keeps growing and the requirement of being at the same time cheap and fully automatable has made failed to most of the processes tried so far.

One of them is the use of *Optical tweezers* (Figure 6a), which focus a laser beam to pinpoint particles to specific positions. Despite the high resolution provided, its cost and complexity is a big disadvantage and it may also affect the particles when used for locating cells. Another method currently being taken into account is the *Dielectrophoretic trapping*, that utilizes the potential polarizability of the target to produce a force through an electric field that traps this particle, as seen in Figure 6b. It allows to control its movement by changing the field gradient. However, the high complexity and negative effects on the cells become a problem for this technique again. Finally, there also exist investigations about some sort of *Magnetic trapping* to use them for microparticles with magnetic properties (Figure 6c. Nevertheless, in spite of not altering the target, its own nature makes the range of its utility too small and only applicable in a few cases.

Meanwhile, there exist other techniques that do not share these limitations, being mainly the *Acoustic* and *Hydrodynamic trapping*. In these cases, the only complexity they may face will be purely mechanical.

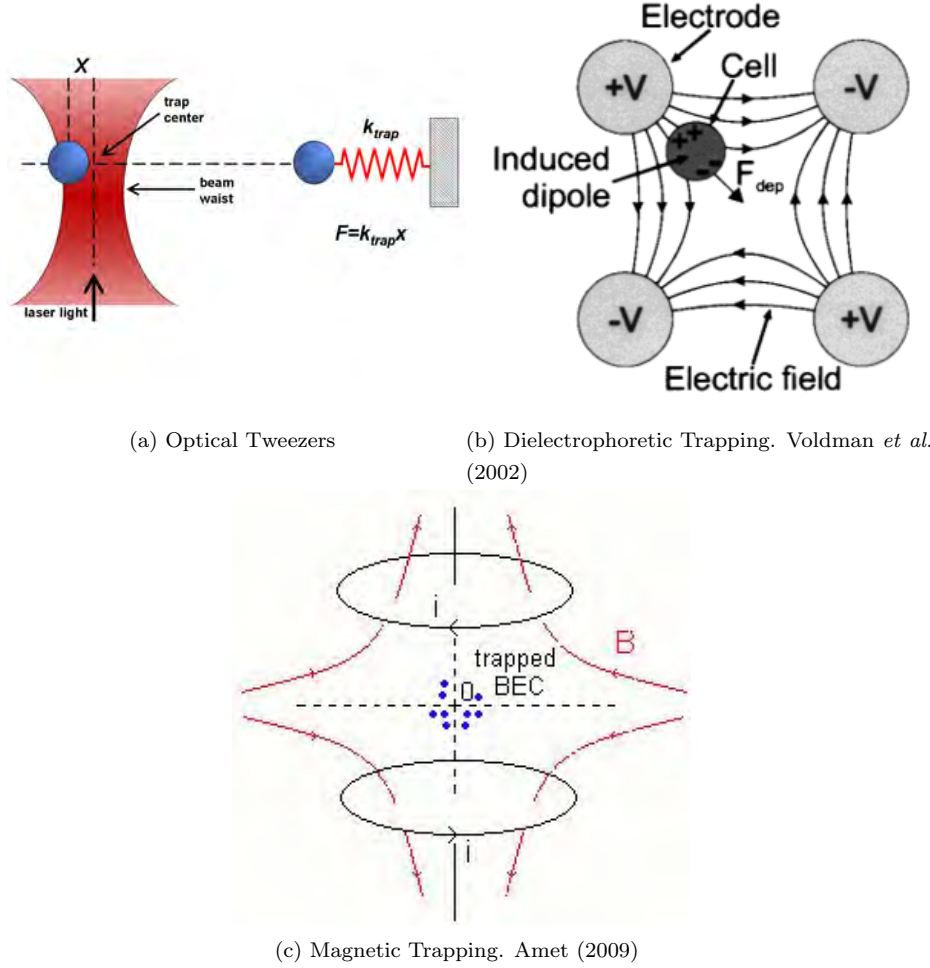


Figure 6: Trapping techniques

In the case of *Acoustic particle trapping*, radiation forces created by the particles when being placed in a standing ultrasonic wave make them move towards the waves nodes, following the distribution in Figure 7. This force depends on the density and compressibility of the targets as well as on the medium in which they are suspended. A piezoelectric transducer is usually in charge of generating the ultrasonic wave whose wavelength will define its spatial resolution. Acoustic tweezers are especially suitable for trapping agglomerations of microparticles.



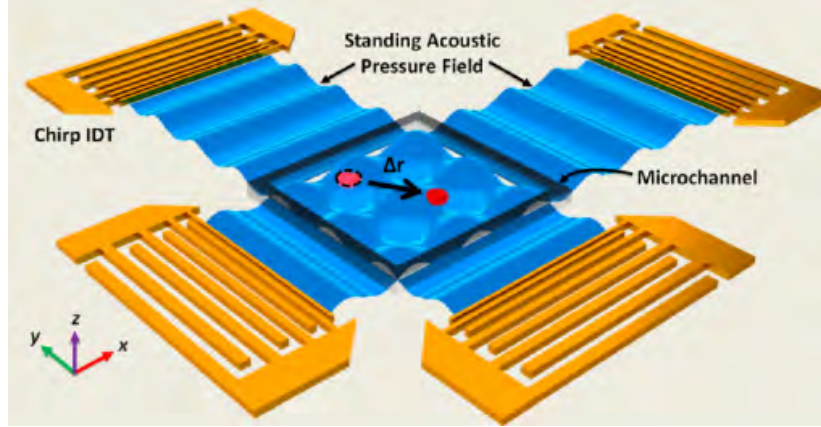


Figure 7: Acoustic particle trapping. Ding *et al.* (2012)

On the other hand, in *Hydrodynamic particle trapping* the micro-particles are pushed to certain spatial positions by the action of flow fields and eventually get trapped in a spiralling trajectory. This is due to a flow configuration called *microeddy*, commonly created by sudden changes in the section or cavities, making them dependent of the flow rate in the channel. So again, its nature makes this method difficult to control.

This is where the steady streaming phenomenon has emerged as a strong option to solve the problem. As another hydrodynamic technique of creating *microeddies*, in this case the strength of these vortices only changes with the amplitude and frequency in the oscillation of a solid body.

#### 1.1.2.b Previous studies

As it has been shown in this project so far, the potential possibilities of the hydrodynamic steady streaming flow are big as well as wide. Knowing this importance, several investigations have tried to enclose the nature of the phenomenon and spot the key factors to control it during the last 50 years. However, each of them have faced the problem from a different angle, getting different results and interesting conclusions.

Firstly, researchers started studying the steady streaming flow by numerical approximations in the late 70s like Riley(1966) and Wang(1968) (already shown

in Figure 1).

Actually, Riley studied steady streaming using different approaches and collaborating with several researchers during the second half of the 20<sup>th</sup> century. In 1966, he made a first numerical analysis of the flow over a sphere using matched asymptotic expansions, arriving to the conclusions shown in the Figure 8, where  $R_M$  is proportional to frequency of the oscillation.

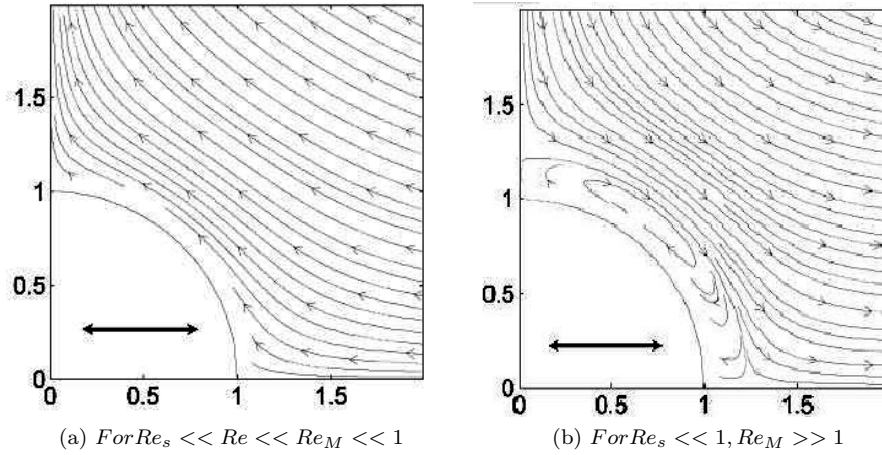
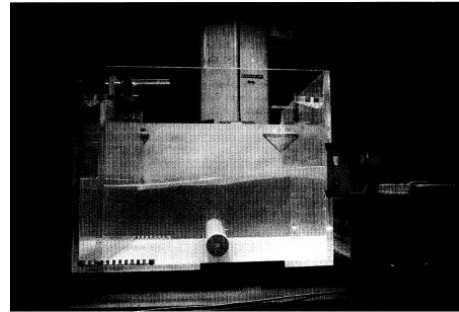
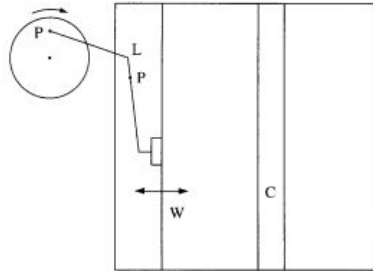


Figure 8: Steady Streaming streamlines over a sphere by Riley (1966)

After this, experiments about this case began to be implemented. Firstly, it was Davidson & Riley (1972) using a vibrating cylinder and later Riley & Wybrow (1995) making use of an elliptic cylinder with different eccentricities. In both cases,  $\varepsilon$  was set between 0.25 and 0.5 while  $Re_s$  was high, within the range of 300-350.

During the year after this last experiment, Wybrow *et al.* (1996) this time focused on the interaction between a cylinder and a rigid wall close to it. For this purpose, the cylindrical body was placed at the bottom of a tank full of water, close to the bottom wall. Meanwhile, on the free surface of the fluid a mechanism using an eccentric disk was spinning and creating waves as shown in Figure 9.



(a) Scheme of the experiment setup. Being P the pivot, L the link, W the wave maker and C the cylinder

(b) Experimental setup

Figure 9: Steady Streaming experiment between a cylinder and a wall by Wybrow, Yan and Riley (1996)

Some interesting conclusions could be extracted from this research that can be apply for real cases were a fixed circular body is placed at the bottom of a mass of fluid that is experienced waves in its free surface. It was noticed that the steady streaming effect induced a recirculating movement to the particles underneath the cylinder, as displayed in the Figure 10, which finally were ejected. This could explain the movement of the seabed covering oil pipelines at the bottom of the oceans.

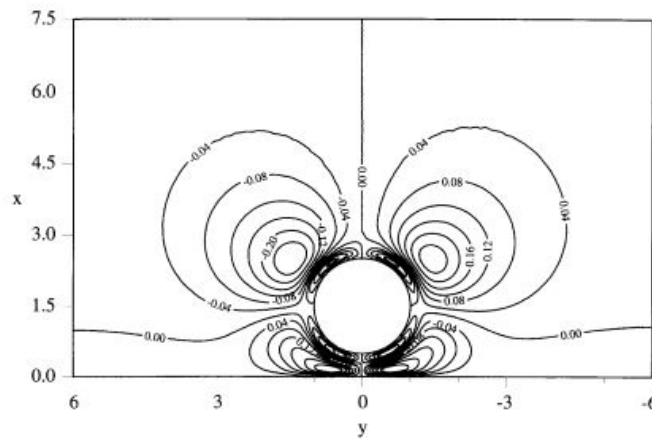


Figure 10: Time averaged streamlines of the Navier-Stokes solution by Wybrow et al (1996)

Another manifestation of the hydrodynamic steady streaming has aroused the interest of researchers during this time, which is inside the hearing system of some fishes. Within it, there is a small otolithic bone full of capillaries that oscillates inside a fluid bag and identifies the amplitude, direction and frequency of the incoming signals (seen in Figure 11).

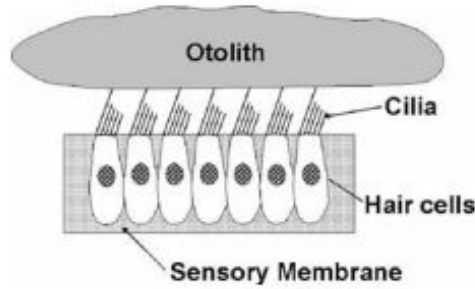


Figure 11: Schematic of the inner hearing system of a fish. Kotas *et al.* (2007)

Kotas *et al.* (2007) performed an fascinating experimental analysis about it, using a spheroid inside a water (10 %) and glycerine (90%) tank as an approximation of the otolithic bone working. As well as in the experiment contained in this project, glass particles were spread all over the fluid and lit while the body is oscillating to capture the progression of the movement. Using values of  $\varepsilon = 0.04 - 1.2$  and  $R_M = 2 - 150$ , the results clearly confirmed the previous numerical studies as shown in Figure 12, as well as agree with the outcome of this project itself.

For the case of two circular cylinders oscillating in parallel, that forms part of this research, Coenen & Riley (2009) achieved a numerical analysis of this situation. This investigation is the basis of this project and it regards a movement with  $\varepsilon \ll 1$  and  $R_s \gg 1$ .

Through the method of asymptotic expansions, different directions of the oscillation movement were studied, depending on its angle  $\phi$  respect to the horizontal axis. For the case that matters to this project, the angle chosen is  $\phi = \frac{\pi}{2}$  and the results display the distribution of the Figure 13.

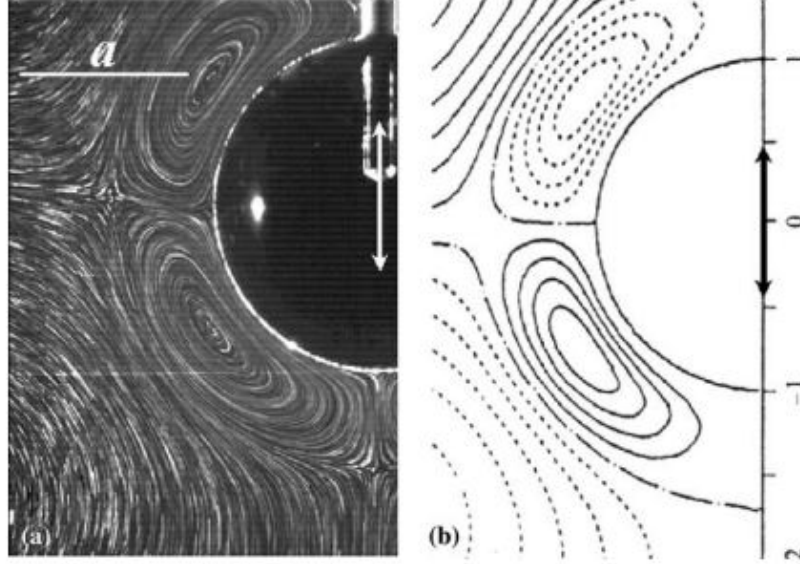


Figure 12: Steady streaming around a vertically oscillated sphere at  $R_M = 84$ ,  $\varepsilon = 0.1$  and  $a = 1.27cm$ . Kotas et al (2007)

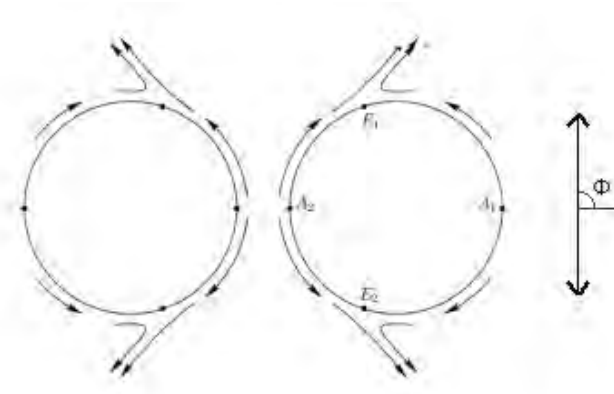


Figure 13: Flow distribution for  $\phi = \frac{\pi}{2}$ .  $\varepsilon \ll 1$  and  $R_s \gg 1$ . Coenen and Riley (2009)

To prove these analytic results, several experiments were made by Galan (2013) with the same lab set-up used for this project. In this way, it could be discovered that the actual direction of the jets produced by the cylinders was towards their centres. This means, against what was previously guessed, that the momentum of the flow facing the ejection point  $E_1$  from the outside is bigger

than the one coming from the inner region, resulting in the direction towards the centre that generates the eddies. Figure 14 shows the results of one of these experimental studies.

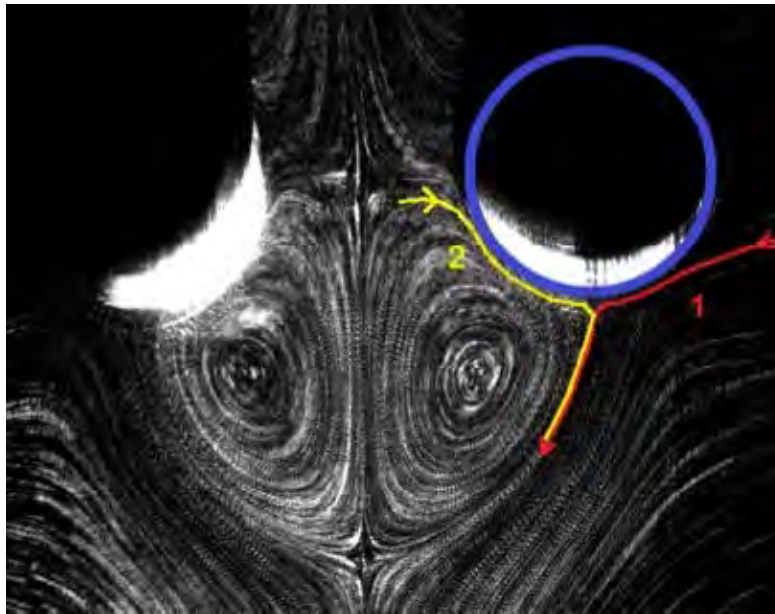


Figure 14: Experimental flow distribution by Galan (2013)

This project is based on all these previous studies achieved during the last 50 years, but as it is seen, the literature about this phenomenon is still young and definitely not complete. The steady streaming has a huge potential and many possible applications for the human being, so it is important to keep researching and analysing the parameters that would lead to control it.

### 1.3 Objectives

This project has the aim to confirm and extend the results obtained by the previous experiments for two oscillating cylinders of Galan (2013) as well as to explore the steady streaming created by a new distribution, formed by four circular cylinders placed in a square. For this purpose, the objectives of this project are:

- Assemble the laboratory set-up for both distributions of cylinders.
- Calibrate the incidental laser beam, the measurement devices and the camera.
- Fulfilment of a series of experiments of steady streaming over two cylinders through a wide range of values for  $Rs$ .
- Fulfilment of two sets of experiments of steady streaming over four cylinders varying the direction of the movement and the value of  $Rs$ .
- Record and post-process the results for each set of experiments.
- Analyse the outcome of the experiments.
- Conclude the meaning of the findings and compare them with the previous theoretical study.

## 1.4 Project plan

This project has been achieved during the first semester of the 2015, from mid January until mid June. This makes a total of 21 weeks for completing the objectives that were set at the beginning.

The work can in turn be divided into four main tasks:

- Study of the theoretical basis (Weeks 1-3)
  - Week 1-2: Investigate the physical base of the *steady streaming*.
  - Week 3: Research and summarize previous studies and experiments.
- Assembly of the lab set-up and first experiments (Weeks 4-14)
  - Week 4-5: Rearrange the tank and the supporting structures.
  - Week 6: Introduce the mixture of glass particles and stir the fluid.
  - Week 7: Align the laser beam with the tank to create a perfect horizontal plane.
  - Week 8-9: Calibrate the camera options (exposure, height and zoom) to capture the area that it is interesting for the study.
  - Week 10: Connect the camera and the electronic control to the computer and synchronise them with the Software program.
  - Weeks 11-13: First testing experiments to identify errors.
  - Week 14: Place two mirrors at the back side of the tank to light the dark areas and enhance the quality of the images.
- Experiments and post-processing (Weeks 15-19)
  - Week 15: Perform the set of experiments A1, A2, A3 and A4.
  - Week 16: Post-process the raw data for experiments type A.
  - Week 17: Perform the experiments B1 and B2.
  - Week 18: Perform the experiments C1 and C2.
  - Week 19: Post-process the raw data from experiments type B and C.
- Analyse the results and conclusions (Weeks 20-21)
  - Week 20: Compare the outcome with previous experiments.
  - Week 21: Write down the conclusions that can be extracted from the results.



## • FORMULATION •

## 2 Formulation

### 2.1 Geometry

As it has been explained in the previous chapter, the geometry of the bodies and their distribution with respect to the induced movement greatly defines the nature of the experiment. Different geometries create distinct variations of steady streaming flow and moreover its position regarding the others affects directly in the parameters governing the phenomenon. As it has been said, with the experiments of this investigation it is desired to explore the scenario for oscillating cylinders with  $\varepsilon \ll 1$  and  $R_s \gg 1$ , so the geometry chosen should confer these characteristics to the movement.

Therefore, the experiments achieved during this project can be separated in two main types, putting the spotlight on the number of circular cylinders acting on it. Moreover, in some cases different positioning was used within the same type of experiment performed.

#### 2.2.1.a Two cylinders

As it has been briefly introduced during the presentation of the phenomenon, to create the steady streaming over two cylinders they should be placed close enough to each other. To generate low values of  $\varepsilon$  it has been chosen to leave a separation between them close to  $D = 2r$ , being  $r$  the radius of the each cylinder. Despite some other cases found in the literature, this time it has been elected to use cylinders of the same size and therefore radius. One of the projections of these experiments is the viability of trapping particles using steady streaming and the symmetry in the distribution seems necessary for these purposes. A scheme of the geometry is shown in Figure 15.

In addition, since the numerical basis used is the analysis by Coenen & Riley (2009) for different values of  $\phi$ , it is important to remark that in all the experiments accomplished  $\phi = \frac{\pi}{2}$  was used. This means the movement was perpendicular to the axis matching both centres.

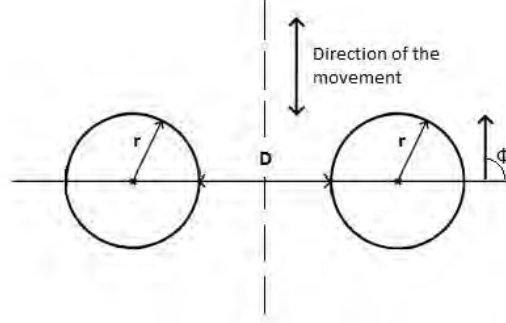


Figure 15: Geometry for experiments using two cylinders

#### 2.2.1.b Four cylinders

During this second series of experiments, now four circular cylinders are placed keeping the same distance between them. This means they are located at each corner of a square with side length  $D = 1.7r$ .

However, to extend the variety of the results, the disk holding the bodies was rotated from one set of experiments to the other. This meant a change in the direction of the movement with respect to the geometry.

**2.2.1.b.1 Distribution 1** Firstly, the square was placed in the way that the direction of the oscillation was perpendicular to two of the sides of its sides. Figure 16 shows a scheme of the geometry.

**2.2.1.b.2 Distribution 2** Secondly, the disc was turned to make the cylinders oscillate in another direction. Now, the movement is perpendicular to the axis matching diagonally the bodies, as displayed in Figure 17. However, the same distances and sizes of cylinders has been used.

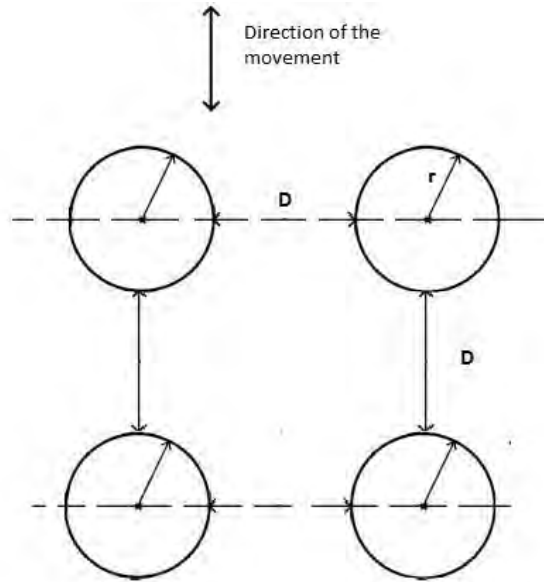


Figure 16: Geometry for experiments using four cylinders. Distribution 1

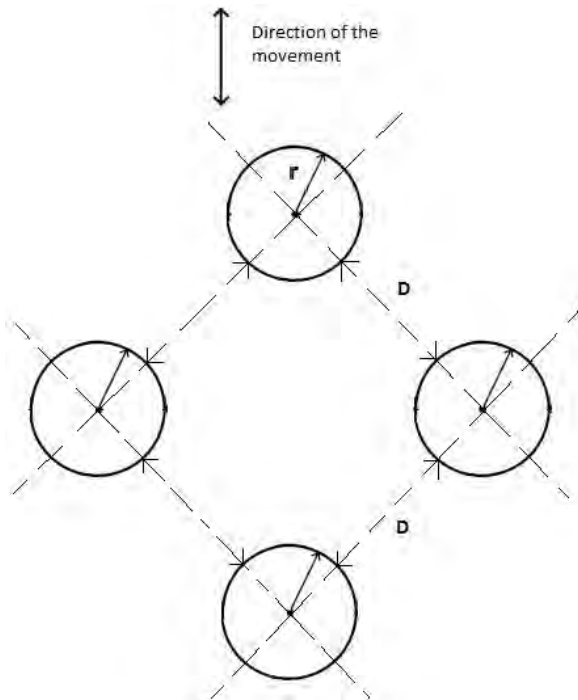


Figure 17: Geometry for experiments using four cylinders. Distribution 2

## 2.2 The movement

Steady streaming is created by the relative movement between a body and a fluid. This sets freedom for the researchers to choose to induce the movement either to the solid or to the fluid. In the case of this experiment, it has been selected to provide the mobility to the cylinders, for simplicity and precision purposes.

Moreover, this displacement must be a linear oscillation to create the desired phenomenon. Therefore, the rotation generated by the electric motor is changed into a swinging linear movement through a mechanical device detailed in the next chapter. This leads to create a sinusoidal move that can be defined as:

$$y(t) = A \sin(\omega t + \psi) \quad (1)$$

Where  $y(t)$  is the vertical position of the cylinders at every instant of time,  $A$  the amplitude,  $\omega$  the angular velocity and  $\psi$  can be assumed to be 0 to simplify the calculations. Despite  $\omega$  can be difficult to measure, the electronic circuit connected to the motor gives the frequency provided and it is known that  $f = \frac{\omega}{2\pi}$ .

Once these parameters are defined, it is possible to establish the instant velocity of the cylinder. This variable is needed to successfully non-dimensionalize the Navier-Stokes equations and solve the numerical problem.

$$u(t) = \frac{dy(t)}{dt}$$

$$u(t) = A\omega \cos(\omega t) \quad (2)$$

Also, it is important to define the maximum speed reached by the bodies during each cycle  $U = A\omega$ . The cylinder will experience this top velocity just when  $\cos(\omega t) = 1$ , so  $t = 0$ , meaning when they are in the middle of the oscillation.

## 2.3 Dimensionless analysis

One of the main objectives of this project is to identify the key parameters governing the steady streaming and analyse their influence in the outcome. Therefore, this section will be dedicated to this task, making use of the parameters defined above and shown in the Figure 18. From now on in this part, every variable with  $*$  is referring to a real parameter and has dimensions while the ones who haven't are dimensionless.

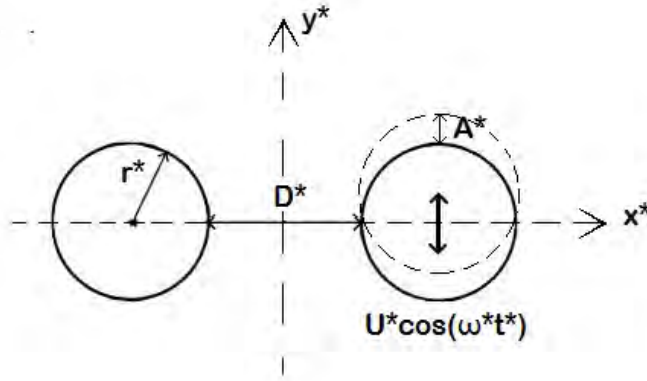


Figure 18: Definition of the real variables

Then, rewriting equations (1) and (2) to fit this criteria:

$$y^*(t) = A^* \sin(\omega^* t^*) \quad (3)$$

$$u^*(t) = \frac{dy^*(t)}{dt^*} = A^* \omega^* \cos(\omega^* t^*) = U^* \cos(\omega^* t^*) \quad (4)$$

Moreover, it is important to define the other acting part of the process, the fluid, whose main characteristics are its viscosity  $\nu$  and density  $\rho$ . It will be also assumed to be incompressible and its only changes in its density are due to perturbations so the pressure instant value can be defined as:

$$p^* = p_m^* + \Delta p^* \quad (5)$$

Now, it is needed to define the non-dimensional parameters that will form the desired expressions. The characteristic values are the radius  $r^*$  for length,  $\frac{1}{\omega^*}$  for time, the maximum velocity  $U^*$  for velocity and  $\rho^* U^*$  for pressure. Making use of them to define the non-dimensional variables:

$$y = \frac{y^*}{r^*} \quad (6)$$

*Non-dimensional position in y-axis*

$$t = t^* \omega^* \quad (7)$$

*Non-dimensional time*

$$u = \frac{u^*}{U^*} \quad (8)$$

*Non-dimensional velocity in y-axis*

$$\Delta p = \frac{\Delta p^*}{\rho^* U^*} \quad (9)$$

*Non-dimensional pressure variation*

$$ga = \frac{D^*}{r^*} \quad (10)$$

*Non-dimensional distance between cylinders*

Once these are defined, it is possible to rewrite the Navier-stokes equation (11) into its non-dimensional form:

$$\frac{\delta u^*}{\delta t^*} + u^* \nabla u^* = - \frac{\nabla^* p^*}{\rho^*} + v^* \nabla^{*2} u^* \quad (11)$$

And introducing equations (7), (8) and (9) into equation (11):

$$\omega^* U^* \frac{\delta u}{\delta t} + \frac{U^{*2}}{r^*} u \nabla u = - \frac{\rho^* U^{*2}}{r^* \rho^*} \nabla \Delta p + \frac{v^* U^*}{r^{*2}} \nabla^2 u \quad (12)$$

Finally, multiplying every term in (12) by  $\frac{r^*}{U^{*2}}$  the equation changes into:

$$\frac{\omega^* r^*}{U^*} \frac{\delta u}{\delta t} + u \nabla u = -\rho^* \nabla \Delta p + \frac{v^*}{U^* r^*} \nabla^2 u \quad (13)$$

As it can be assured, the equation (13) is already non-dimensional and explains the movement of a particle within the fluid during the process. If it is analysed in depth, it can be seen that within equation (13) there appear two characteristic parameters common in the fluid mechanics field:

$$\frac{1}{\varepsilon} = \frac{\omega^* r^*}{U^*}$$

$$\frac{1}{Re} = \frac{v^*}{U^* r^{*2}}$$

However, as it has been mentioned before, this project is focused on the steady streaming movement, so what it turns more interesting is the study of the net movement of the particles only paying attention to the variation of their position after each cycle. To obtain the expression describing this move, it is needed to apply the method of asymptotic expansions implemented by Riley (2001), when  $\varepsilon \ll 1$ , arriving to:

$$u \nabla u = -\nabla(\Delta p) + R_s^{-1} \nabla^2 u \quad (14)$$

This means that at the end, the key parameter to define the steady streaming movement is the streaming Reynolds number  $R_s$ , which contains also the non-dimensional oscillating amplitude  $\varepsilon$ .



- EXPERIMENTAL  
PROCEDURE •

## 3 Experimental procedure

### 3.1 Procedure

The experiments that formed the basis of this project were made in the UC3M Thermal Engineering and Fluids Department laboratory, following the experimental set-up explained below.

The aim was to recreate the conditions of the previous numerical studies achieved by Dr. Coenen and capture the movement of the fluid with a high speed camera for a later processing of the images. For this project, it was also necessary to have freedom to vary the key parameters of the movement, as long as the distribution of the cylinders, to obtain results for different situations.

The experimental set-up, whose components will be explained in detail in this section, was mainly formed, as displayed in Figure 19, by a tank full of water (1) where the cylinders (2) were introduced, the mechanical structure (3) which moves these cylinders using an electric motor (4), a laser (5) that creates an horizontal plane in the water and a camera (6) connected to a computer for collecting the raw data.

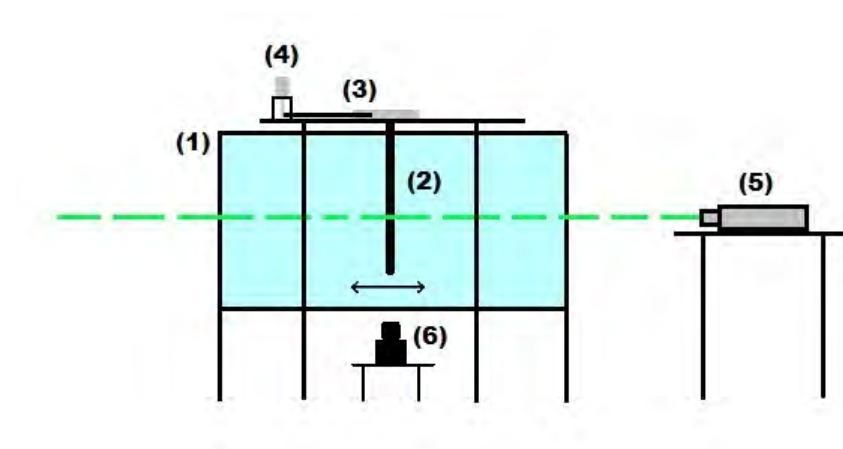


Figure 19: Scheme of the laboratory set-up

Prior to each experiment, the main conditions influencing them were written down. such as temperature, time since the fluid hasn't been stirred, amplitude

of the movement, frequency, duration of the experiment, etc. It is important that the fluid within the tank is free of residual movements that may have been induced if the fluid has been stirred.

The aim of the lab set-up is to create a flux of particles moving within the tank which the camera should be capable of capturing. For this purpose, a laser is placed a few metres away from the tank. It projects, through a lens, a light beam that penetrates the tank and creates a visual horizontal plane crossing at the middle of the cylinders. The water has been previously mixed with glass particles *Sphericell 110P8* for experiments type A and *Vestosint 2159* for B and C, which reflect the incoming light and outline the desired shape of the fluid movement.

The cylinders are introduced in the tank from the top and connected to an electric motor through a mechanical device that transforms its rotation into a linear movement. An electronic circuit is also connected to this system to provide an accurate measurement of the frequency of the oscillation to the camera software for later purposes.

Once the bodies are oscillating and the visual plane is generated, the camera is already able to capture the phenomena occurring inside. It is placed underneath the tank supported by a jack that can adjust its separation from the floor. Depending on the type of experiment desired, the software *INSIDE 4G®* orders to take pictures every given time period or synchronise the camera trigger with a characteristic moment of the oscillation, guided by a signal from the electronic control. For the purposes of this project, capturing the variation on the point where the linear movement reaches its maximum amplitude is particularly interesting and shows the pursued steady state phenomenon.

After getting this raw data of the experiment in the form of images, they are processed by Matlab codes programmed by Dr. Coenen, first of them to skim the glass particles reflection from the residual noise of the ambient light or the cylinders themselves. Once the pictures are clean, they are processed again to gather 8 consecutive images to create small streamlines from the points taken.

## 3.2 The setup

### 3.3.2.a Tank and support system

The tank is made of five transparent methacrylate panels, joined together and hermetically sealed with silicone, leaving the top face open. It is supported by a metallic structure and raised to let space to place the camera underneath it. Also a table with a circular hole in the middle is put above the tank, acting as a support system to place the cylinders and the mechanism that moves them.



Figure 20: Water tank and support system

The tank has a capacity of 160 litres. It is full of water and glass particles in charge of reflecting the light from the laser. The particles should have a density similar to the water for creating an homogeneous mixture along the height of the tank.

To enhance the quality of the images taken, the sides of the tank are covered by a black surface only leaving a rectangular slit for the laser beam to enter.

Induced movements in the surface water may interfere in the results taken, so a foam board is placed floating on the fluid to absorb this movement caused by the cylinders.

Moreover, as it will be explained later, two mirrors are attached to the back of the tank to reflect part of the laser beam passing through the bodies. In this way, some of the area covered by the shadow of the cylinders themselves will be lit, providing a wider vision of the phenomenon.

### 3.3.2.b Laser

The laser used to create the visual plane that the camera is able to capture is the model EXLSR-531-300-CDRH developed by Lasing s.a. It has a wave length between 300 and 2000 nm and emission energy of 400 mJ.

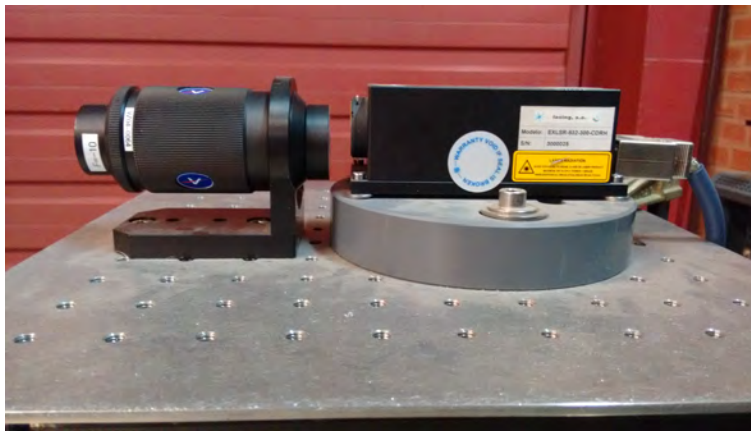


Figure 21: Laser

The transmitting laser just creates a linear beam so, to generate a plane, a quartz lens has been connected to the laser exit. This projects the beam in a divergent plane that enters the tank and impacts on the middle of the cylinders.

However, the bodies themselves produced a shade in the area behind, making it impossible for the camera to capture this region. This was one of the problem of the previous experiments that formed the base of this project. In the Figure 23, the region I represent the area captured by the camera and II the dark zone unable to study.



Figure 22: Laser emitting

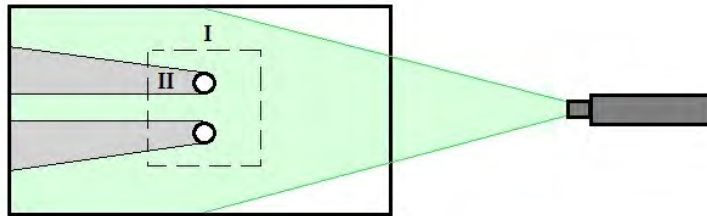


Figure 23: Laser plane regions

To improve this, two mirrors were placed at the back of the tank to reflect the portion of the beam that pass through between the cylinders and light up the dark areas, as displayed in Figure 24.

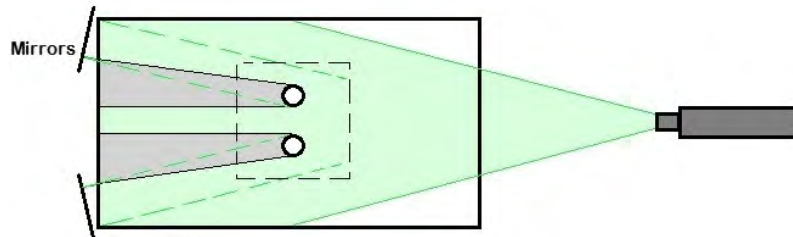


Figure 24: Laser plane regions with the mirrors

### 3.3.2.c Motor

An electric DC motor has been used to transmit the power for the movement of the cylinders. It can deliver a voltage between 4.5 and 15 V and 21.2W.



Figure 25: Electric Motor



Figure 26: Voltage generator

The motor is fed by a power source that provides a range of 0-30V. A variation in this voltage directly changes the frequency of the movement. This permitted to study different cases depending on the velocity of the cylinders.

### 3.3.2.d Cylinders

In the experiments made during this project, two different distributions of cylinders have been used.

The first one was formed by two solids separated from each other (Figure 27). With this distribution, the aim was to confirm the results obtained in previous studies and get a better resolution of the experiment.



Figure 27: Distribution for two cylinders



Figure 28: Distribution for four cylinders



The second one contained four cylinders forming a square (Figure 28). There are no previous experimental studies about this distribution but due to its symmetry, it is interesting to analyse how the results change with this new geometry.

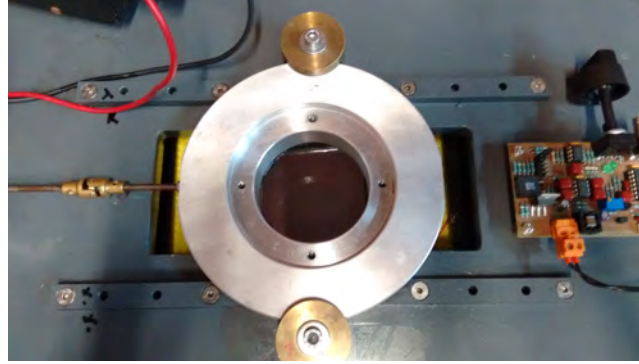
All of the cylinders used were pre-treated with a matt black paint coat. This helped avoiding the reflection of the light once it hits the bodies, providing a better image of what it is indeed interesting, the particles within the fluid.

### 3.3.2.e Movement transmission

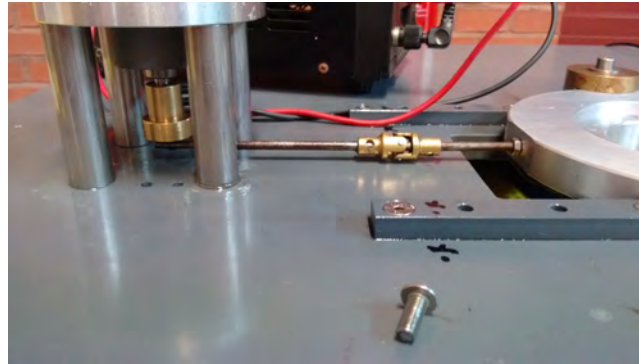
As it can be seen in Figure 27 and 28, the bodies are attached to a circular metal plate. This one fits inside another plate of bigger radius that is allocated between two rails that only allow the linear movement of the piece. This is then attached through a connecting rod to a crank that converts the circular movement of the electric motor into a steady linear oscillation.

Indeed, the main weaknesses of this experimental set-up that may cause errors in the results is the clearance in the transmission. This results in a variation in the real amplitude of the movement that will be taken into account in the experimental procedure. Using the images taken by the camera, it is possible to find out graphically the real displacement the cylinders describe. This will help to calculate more accurate values for  $\varepsilon$  and  $R_s$ .

So one of the main ways to improve the results for future experiments is changing the transmission of the movement from the electric motor using devices with smaller tolerances. This would decrease also the variability in the amplitude between cycles, helping to stabilize the steady streaming movement as well.



(a) Cylinder connection to the movement transmission



(b) Transmission

Figure 29: Oscillation movement transmission

### 3.3.2.f Electronic control

As it will be explained in detail, for the right identification of the steady streaming movement it is needed to gather frames of the location of the particles at the same exact time every cycle.

This means the camera must take pictures every fixed period of time that depends on the frequency of the movement provided by the motor. This is the task of the electronic integrated circuit connected between the computer and the motor. It measures the period of the oscillation at which the bodies are moving and sends a trigger signal to the computer.

Moreover, depending on what particular part of the cycle we are interested in, it has an offset regulator to adjust when it delivers the order. This means it

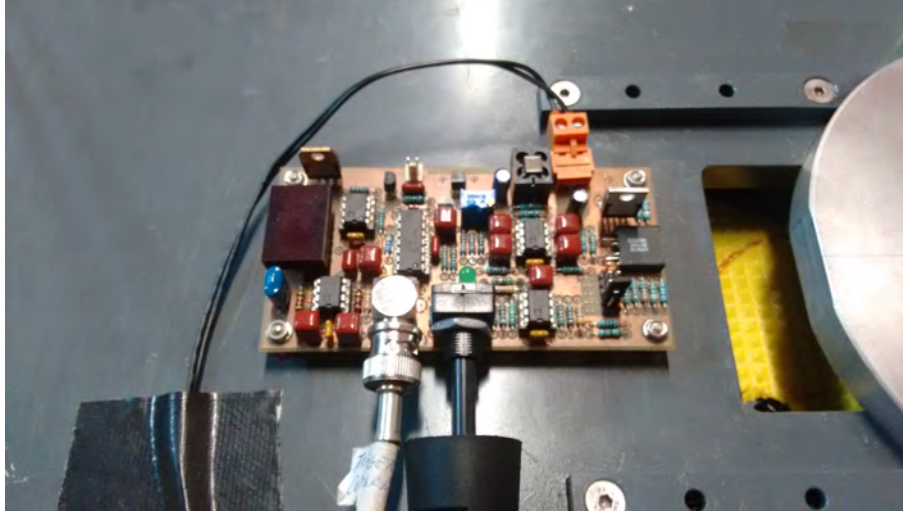


Figure 30: Electronic circuit

is possible to study the steady streaming net movement focusing on the moment when the cylinders are in their maximum amplitude or change it to study when they experience the biggest velocities.

### 3.3.2.g Camera and software

To capture the phenomenon happening in the fluid, it is needed a device able to capture many pictures in a small period of time. The camera chosen was the model XMV-2M-CL, which is capable of taking up to 30 frames per second. Moreover, it has an input to plug in the trigger cable that delivers the command of capturing the picture.

By this, it is connected directly to the computer which, through the software program INSIDE 4G®, coordinates all the actions. This program is able, using the information given by the electronic control, to activate the camera trigger at the same point of every cycle and gather the raw data. It also allows to vary graphic options of the image, as the exposure, and change between free and synchronised trigger mode.



Figure 31: Camera set-up



Figure 32: Camera

### 3.3 Image processing

During the experiment, the camera keeps taking photos when the software program INSIDE 4G® activates the trigger. These images show the light reflected by the particles in the plane of study. However, it is needed to somehow relate the raw pictures between them to find out the progression of the position of each glass particle. This was achieved by post-processing the whole set of raw data using the Matlab codes developed by the tutor of this project, W. Coenen.

Firstly, it is essential to remove all the visual noise that negatively affects the vision of the particles. Even though the tank has been covered, the cylinders are coated with matt black paint and the lights were turned off during the experiments, some residual light is still reflected by parts of the set-up that are not interesting for the research. In order to get rid of it, the Matlab code *subtractmin* gathers 8 photos together and compares them. Then, all the elements that have stayed constant during this set of pictures are considered irrelevant and separated from the moving elements.

Therefore, the program generates two different files from every raw element of data. The first one, as it is shown in Figure 33, it contains all the visual noise from light emitted by the cylinders and reflections generated by the tank walls. Meanwhile, in the other file there is only the particles which have been constantly moving during the period taken. The Figure 34 is an example of the clean outcome image achieved after applying *subtractmin* program.

After executing this first code, the data show a clean image showing just the important information, however the pictures could not be ready to analyse. Even though the camera has been adjusted to achieve this, the final outcome may not be perfectly aligned causing some asymmetry that is interesting to reduce.

Moreover, it might be useful to identify graphically the solid cylinders in every picture. The code *findcylinders* is responsible for both tasks. Using a clean image as a reference, the code allows to select points of the cylinder contour and use them to draw its circumference over the photo, as in Figure 35.

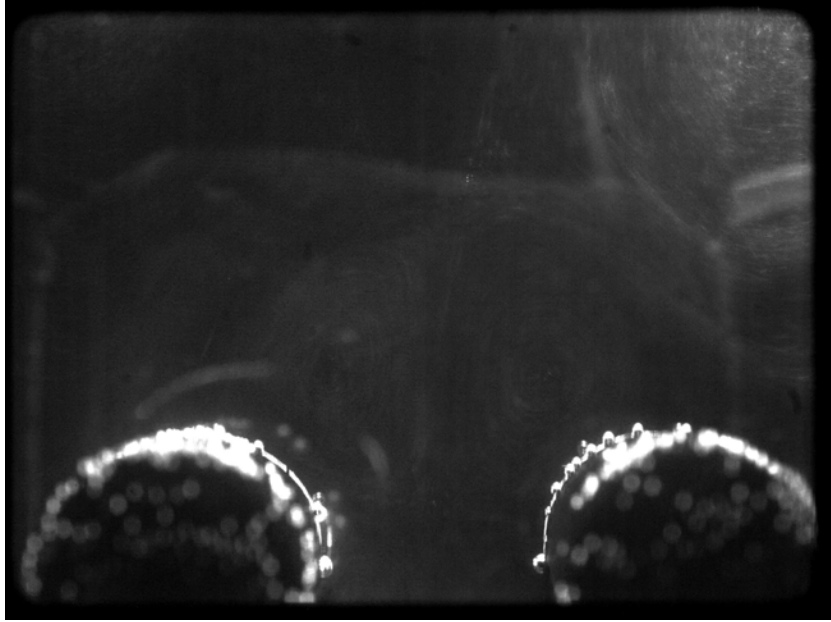


Figure 33: Visual noise contained in the raw images



Figure 34: Clean processed image



With this information, *findcylinders* is able to correct the deviation in the alignment of the cylinders and give a perfect symmetric image.



Figure 35: Identification of the cylinders

Finally, the pictures are prepared to be processed and generate a global view of the steady streaming movement. The Matlab program *streaklines* is on charge of this, forming the final stage of the post-process procedure. It basically uses a given number of images (in this case 16) to superimpose the different positions of the particles during this period of time.

This uncovers the real movement patterns that the fluid is describing and permits to recognise the steady streaming characteristic structures. Figure 36 shows an example of the streamlines that this code generates as outcome.

As it can be seen, after applying these three Matlab codes the raw data taken goes from a random collection of point and reflection into a easily recognisable



Figure 36: Streamlines during steady streaming

steady streaming flow structure.

Nonetheless, *streaklines* also offers another interesting option to completely understand the results. This code can use the set of images that has created to superimpose them and produce a video file that gives a dynamic overview of the particles movement. This allows to check the position of the characteristic stagnation points and vortices through time and see if they stay constant in the space. This would be desired for particle trapping applications.



## • Results •

## 4 Results

As it has been mentioned in the objectives of this project, the experimental section is divided in two main groups. One of them gathering analysis of the case where two cylinders are moving (type A), the other one when they are four. In addition, within the second group it can be found experiments type B and C.

Moreover, within each type of test, several runs have been made varying the key parameters between them. The main variable, whose relevance is wanted to be studied, was the streaming Reynolds number  $Rs$ . Therefore several experiments were made increasing this non-dimensional number as it will be described in this section.

Nonetheless, it is important to mention that experiments using four cylinders haven't been found in the literature. Therefore, two directions for the movement were analysed, modifying the orientation of the cylinders regarding the oscillation generated. So it was possible to investigate two different approaches of the steady streaming for this unexplored distribution.

### 4.1 Experiments with two cylinders

For this set of experiments the main objective was to obtain a wide range of results for different situations when two cylinders are placed, as well as a good quality on them. To get this variety, as it has been said in previous chapters, it is needed to modify the key parameters  $Rs$  and  $\varepsilon$ . However, it is always crucial to have a small value for  $\varepsilon$  to avoid problems like separation of the boundary layer, so it was kept constant during the whole set of experiments. Meanwhile, the  $Rs$  was increased in each run, through a raise in the frequency of the electric motor movement.

The main set of experiments with this distribution was made consecutively to avoid errors in the measurements due to the transitory stage. Doing it this way, the velocity of the movement was increased gradually between runs. A graph of the procedure followed to make the runs is shown in Figure 37.

Even so, the first moments after increasing the velocity, the process is within a stationary stage while the particles start moving and they get fully affected by the oscillation of both cylinders. Firstly, (Figure 38) the fluid describes irregular patterns and starts drawing the shape of the recirculating cells (Figure 39). After a certain time, the stagnation point between cylinders becomes noticeable as it is seen in Figure 40 and finally the full vortex structure of the steady streaming movement is stable as in Figure 41. At this stage, the experiments could then be started.

Since this project focuses on the net steady streaming movement of the fluid, the camera trigger was synchronised with the movement of the bodies. More experiments were made during this research setting the trigger free and capturing 30 frames per second, but they haven't been included in this report because of their absence visual relevance.

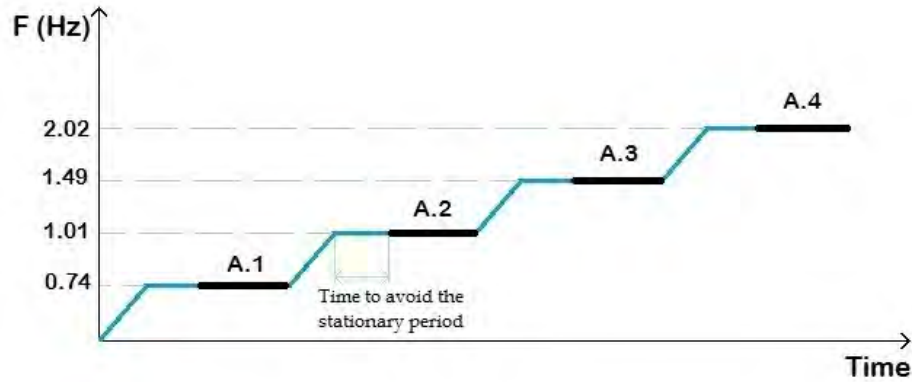


Figure 37: Set of experiments Type A

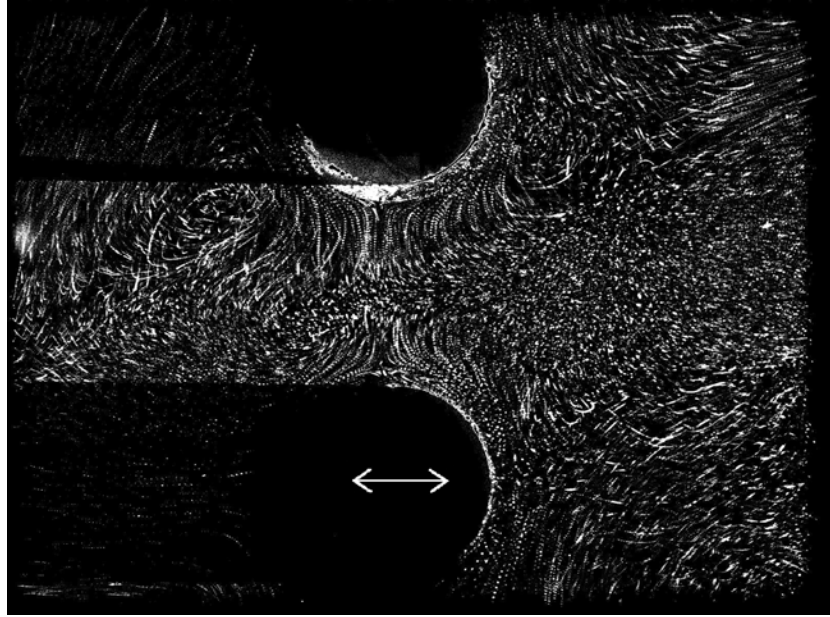


Figure 38: Stationary period at  $t_1$ . Experiment for  $Rs = 155.16$   $\varepsilon = 0.14$

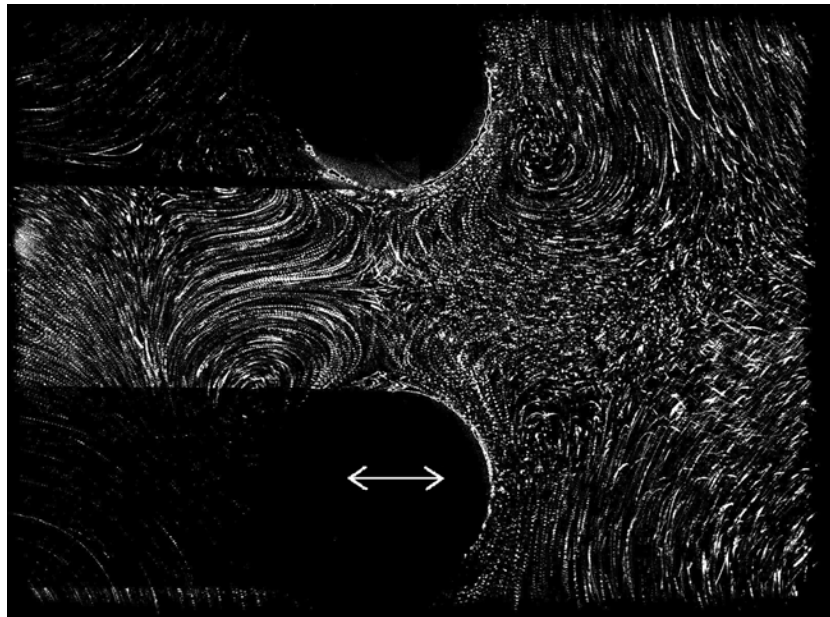


Figure 39: Stationary period at  $t_2$ . Experiment for  $Rs = 155.16$   $\varepsilon = 0.14$

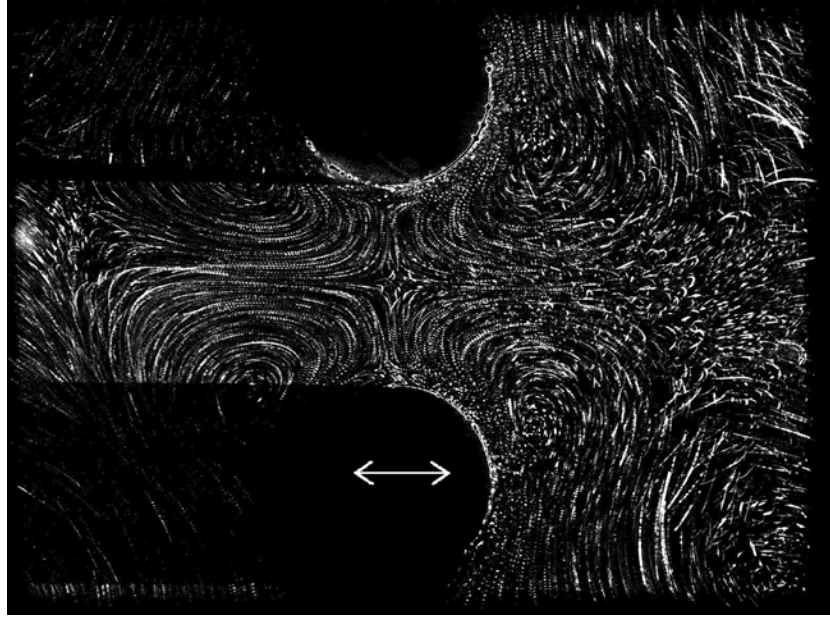


Figure 40: Stationary period at  $t_3$ . Experiment for  $Rs = 155.16$   $\varepsilon = 0.14$

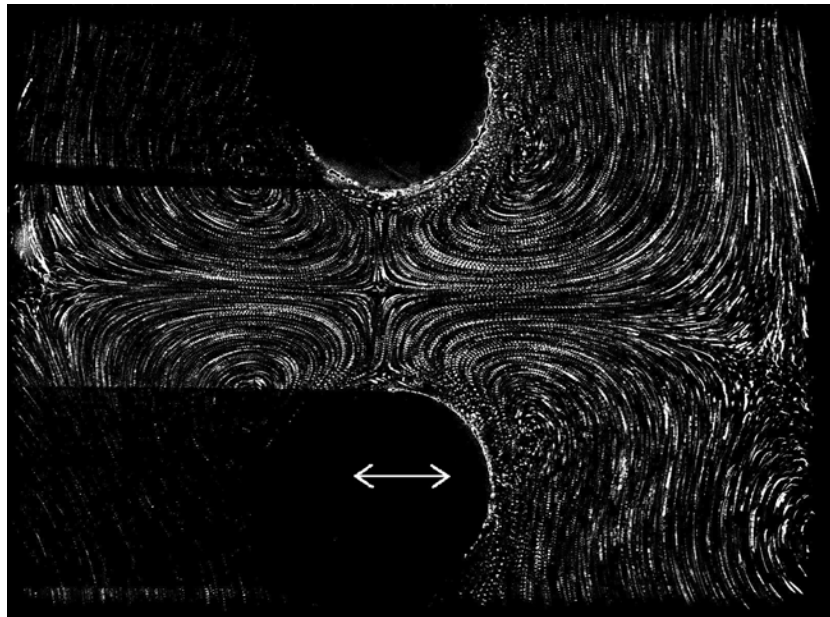


Figure 41: Stationary period at  $t_4$ . Experiment for  $Rs = 155.16$   $\varepsilon = 0.14$

It is important to mention that, as in any scientific experimental procedure, some error is inherent to the method. As it has been briefly introduced in the previous chapter, it is due to clearances in the transmission of the movement to the cylinders and also caused errors in the measurements of the geometry. To minimize this deviation, both oscillation amplitude and radius have been sized mathematically through the graphic results. The Figure 42 gathers the real geometry parameters that were kept constant during the different experiments.

| <b>Constant Parameters</b>      |                |
|---------------------------------|----------------|
| <b>r</b>                        | <b>10.5 mm</b> |
| <b>A</b>                        | <b>1.45 mm</b> |
| <b><math>\varepsilon</math></b> | <b>0.14</b>    |
| <b>ga</b>                       | <b>2</b>       |

Figure 42: Real geometry parameters for experiments type A

Using these real quantities, it is possible to obtain a more accurate value for  $R_s$  and  $\varepsilon$  that will characterize better each case. Figure 43 shows the variables that describe each case calculated for the real geometry of the distribution.

| <b>Experiment</b> | <b>Trigger mode</b> | <b>Photos</b> | <b>Frequency</b> | <b><math>R_s</math></b> |
|-------------------|---------------------|---------------|------------------|-------------------------|
| A.1               | Synchronised        | 1500          | 0.74 Hz          | 71.76                   |
| A.2               | Synchronised        | 1500          | 1.01 Hz          | 97.94                   |
| A.3               | Synchronised        | 1500          | 1.49 Hz          | 144.49                  |
| A.4               | Synchronised        | 1500          | 2.02 Hz          | 195.89                  |

Figure 43: Parameters for experiment type A



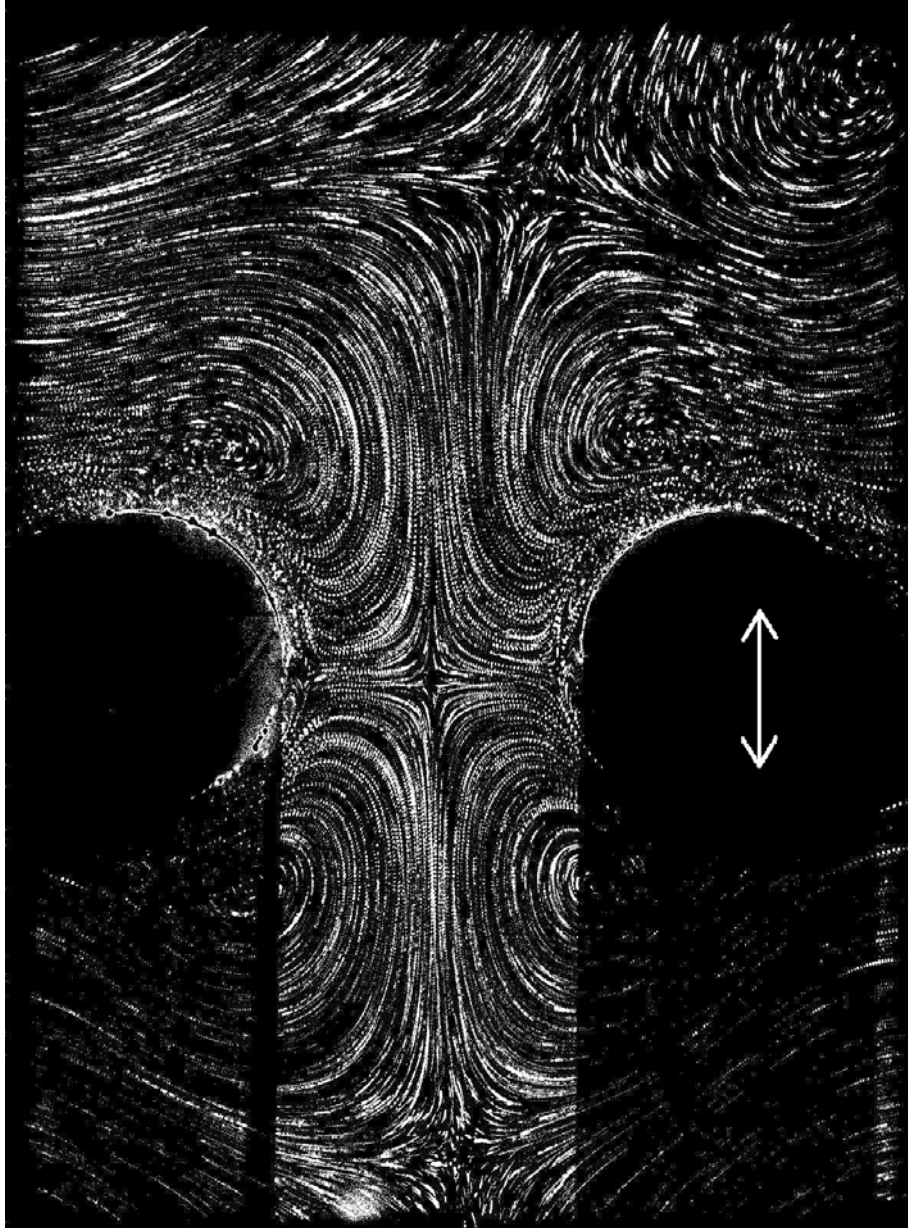


Figure 44: Streamlines distribution. Experiment A1:  $\varepsilon = 0.14$  y  $Rs = 71.76$

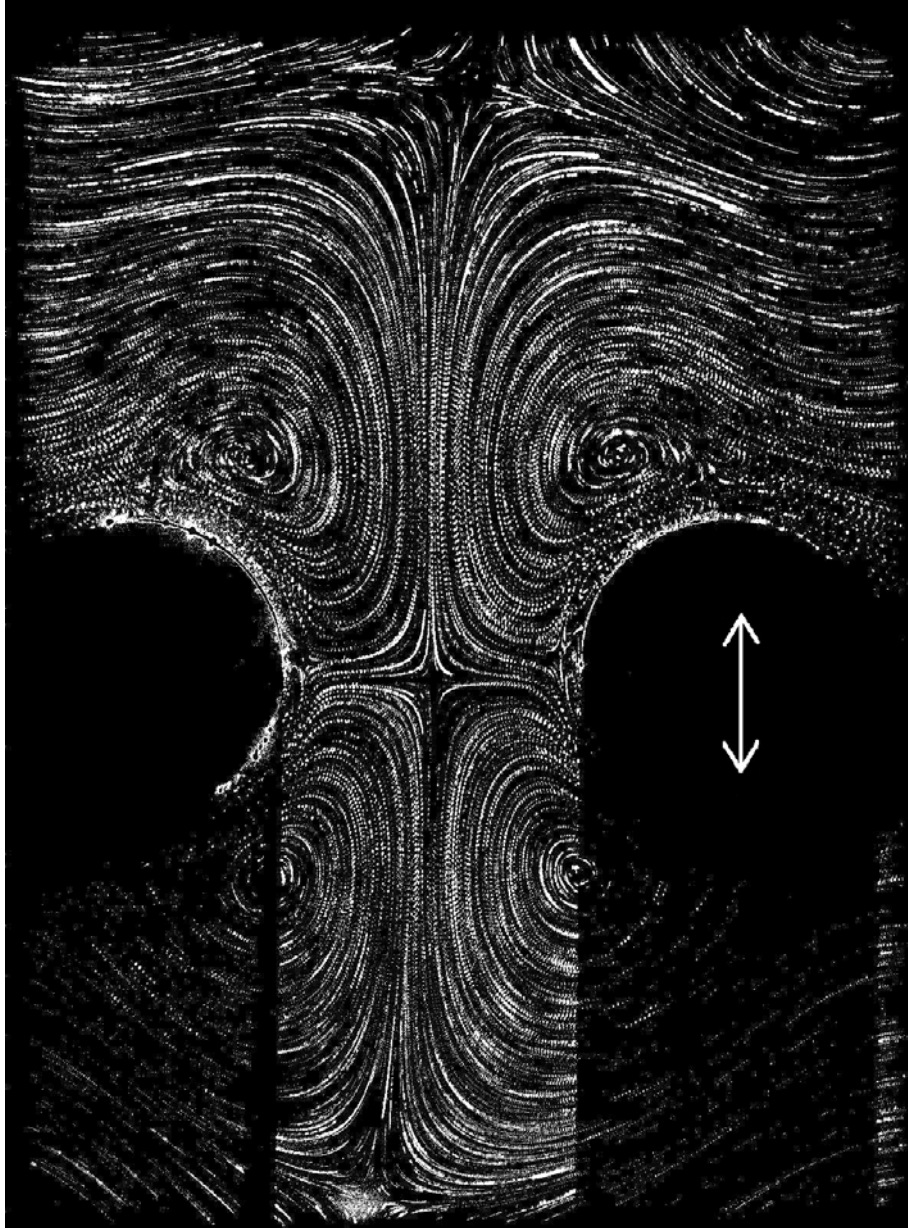


Figure 45: Streamlines distribution. Experiment A2:  $\varepsilon = 0.14$  y  $Rs = 97.94$



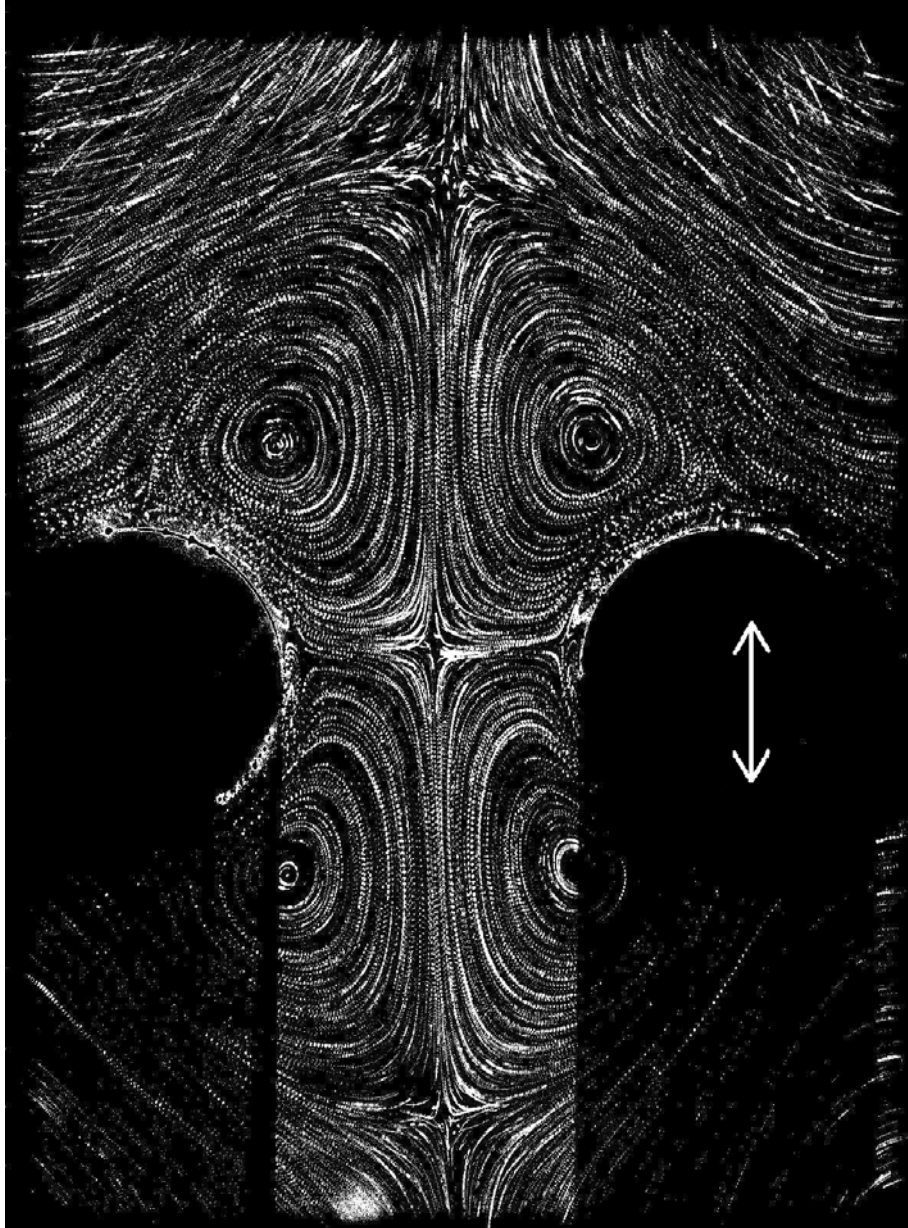


Figure 46: Streamlines distribution. Experiment A3:  $\varepsilon = 0.14$  y  $Rs = 144.49$

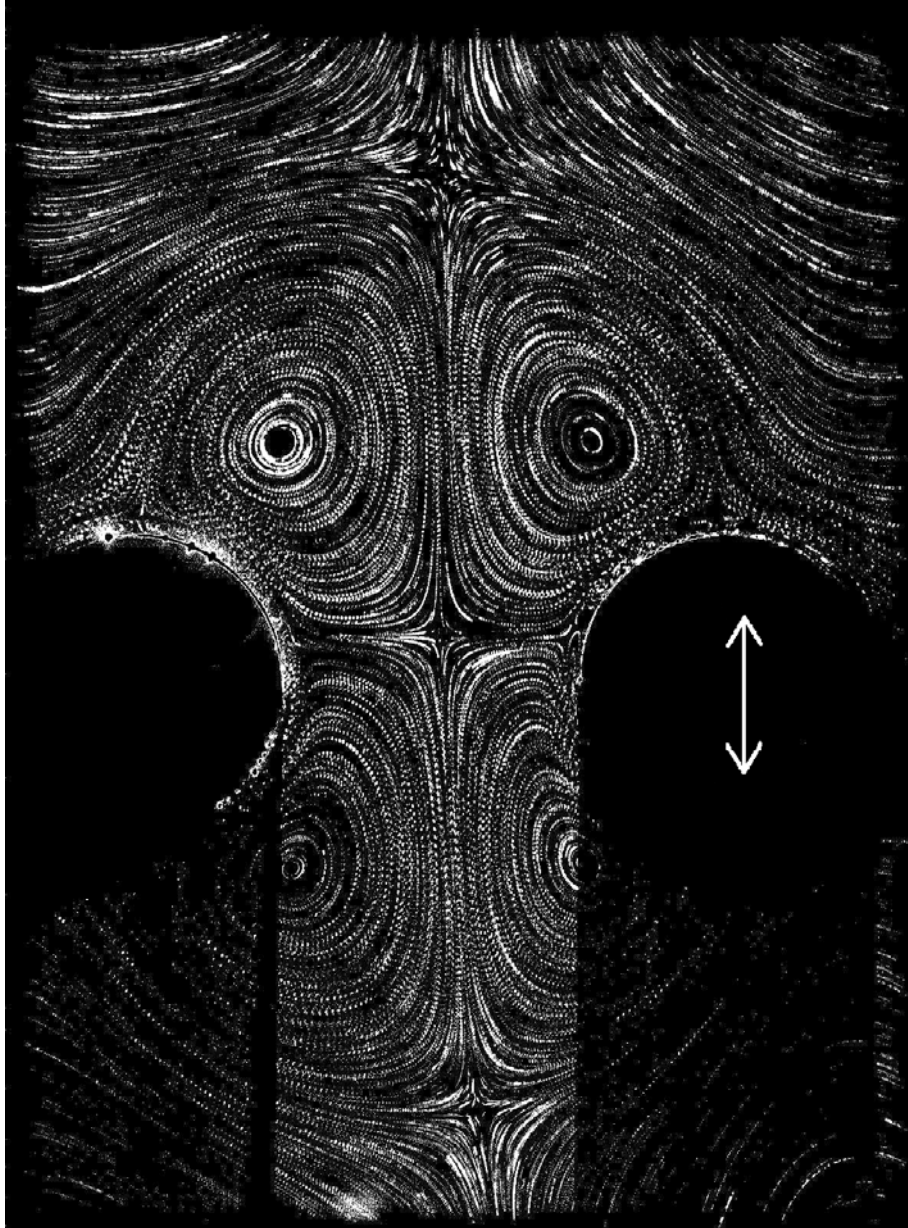


Figure 47: Streamlines distribution. Experiment A4:  $\varepsilon = 0.14$  y  $Rs = 195.89$

## 4.2 Experiments with four cylinders

The second section of the experimental part of this project involved the analysis of the steady streaming produced over 4 oscillating cylinders. For this reason, two new cylinders of the same size were added to the disk that holds the oscillating bodies. This piece had to be modified to leave space for the new solids and they were placed forming a square, as shown in Figure 28.

It is also interesting to mention that, despite studies using this distribution of cylinders are not present in the literature, it would be reasonable to find some similarities with the experiment using two cylinders. Since the radius of the new bodies are the same, as well as the amplitude provided by the motor, both experiments share the same non-dimensional oscillation amplitude  $\varepsilon$ . A similar range of frequency was used, meaning also that the streaming Reynolds number  $Rs$  was equivalent too. However, the distance between them  $C$  and its non-dimensional equivalent  $ga$  is smaller in this case. The new parameters that are common to experiments type B and C are shown in the Figure 48

| Constant Parameters |         |
|---------------------|---------|
| $r$                 | 10.5 mm |
| $A$                 | 1.45 mm |
| $\varepsilon$       | 0.14    |
| $ga$                | 1.7     |

Figure 48: Real geometry parameters for experiments B and C

However, the vortices induced by the movement that are supposed to be created in the region between the cylinders are now much more constrained. In this case, the area right in the middle is surrounded by four solid bodies, so it is logical to expect stronger vortices and bigger trapping capabilities.

In addition, two different types of experiments have been made for the steady streaming over four cylinders. The first one, from now on called Type B, was executed placing the square formed by the cylinders with its sides perpendicular to the movement direction. In the other hand, the experiment Type C

was performed disposing the bodies forming a diamond, by turning them  $45^\circ$  from the horizontal axis. Schemes of both distributions were displayed at the Formulation section of this project, in Figures 16 and 17.

The Figure 49 gathers the parameters that characterize the experiments made for analysing the steady streaming over four cylinders.

| Experiment | Trigger mode | Photos | Frequency | Rs     |
|------------|--------------|--------|-----------|--------|
| B.1        | Synchronised | 400    | 1.74 Hz   | 168.74 |
| B.2        | Synchronised | 400    | 1.74 Hz   | 168.74 |
| C.1        | Synchronised | 400    | 0.76      | 73.70  |
| C.2        | Synchronised | 400    | 1.73 Hz   | 167.77 |

Figure 49: Parameters for experiments B and C

It is also interesting to mention that experiments B.1 and B.2 differs in the proportion of glass particles in the water tank. For run B.2 more *Vestosint 2159* particles were added to enhance the visibility, moreover in the dark areas behind the cylinders.



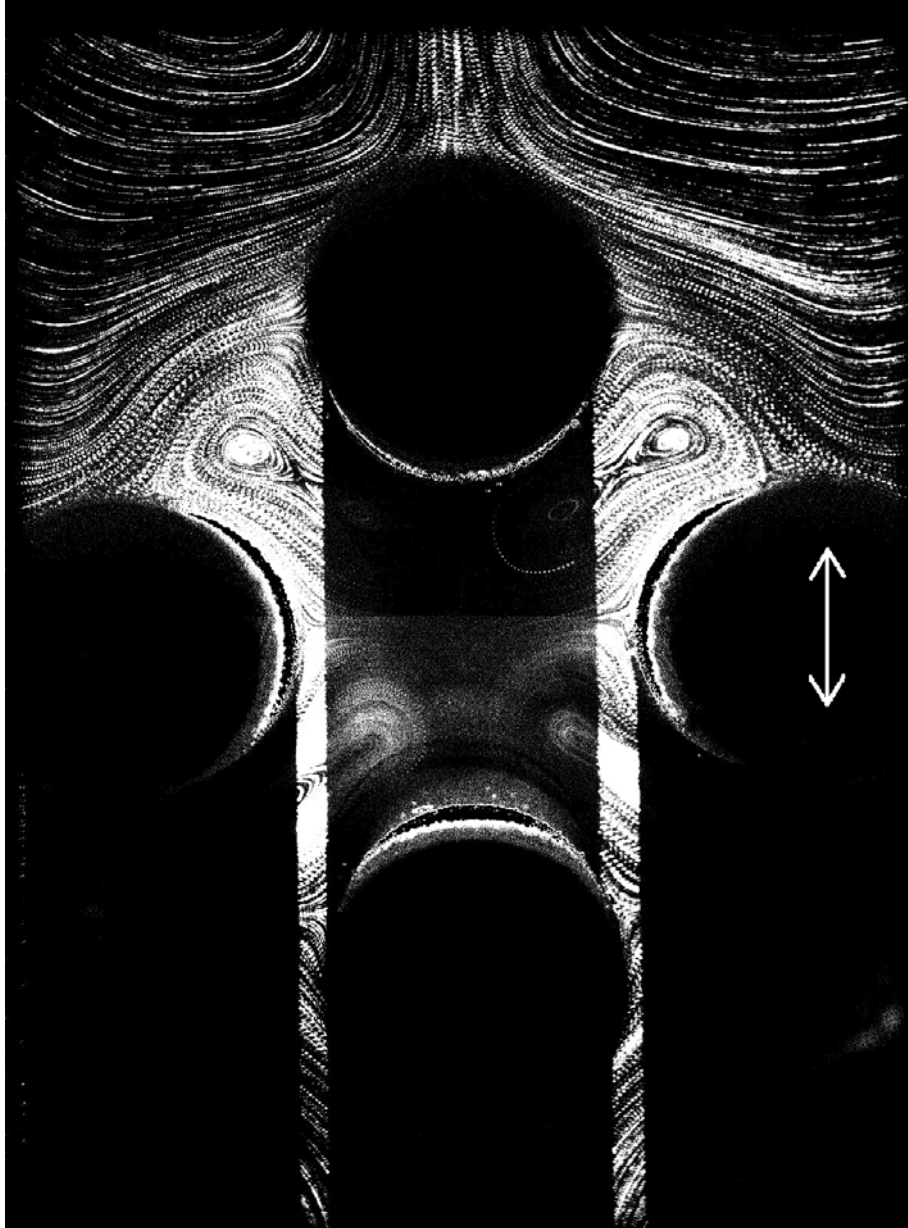


Figure 50: Streamlines distribution. Experiment B1:  $\varepsilon = 0.14$  y  $Rs = 168.74$

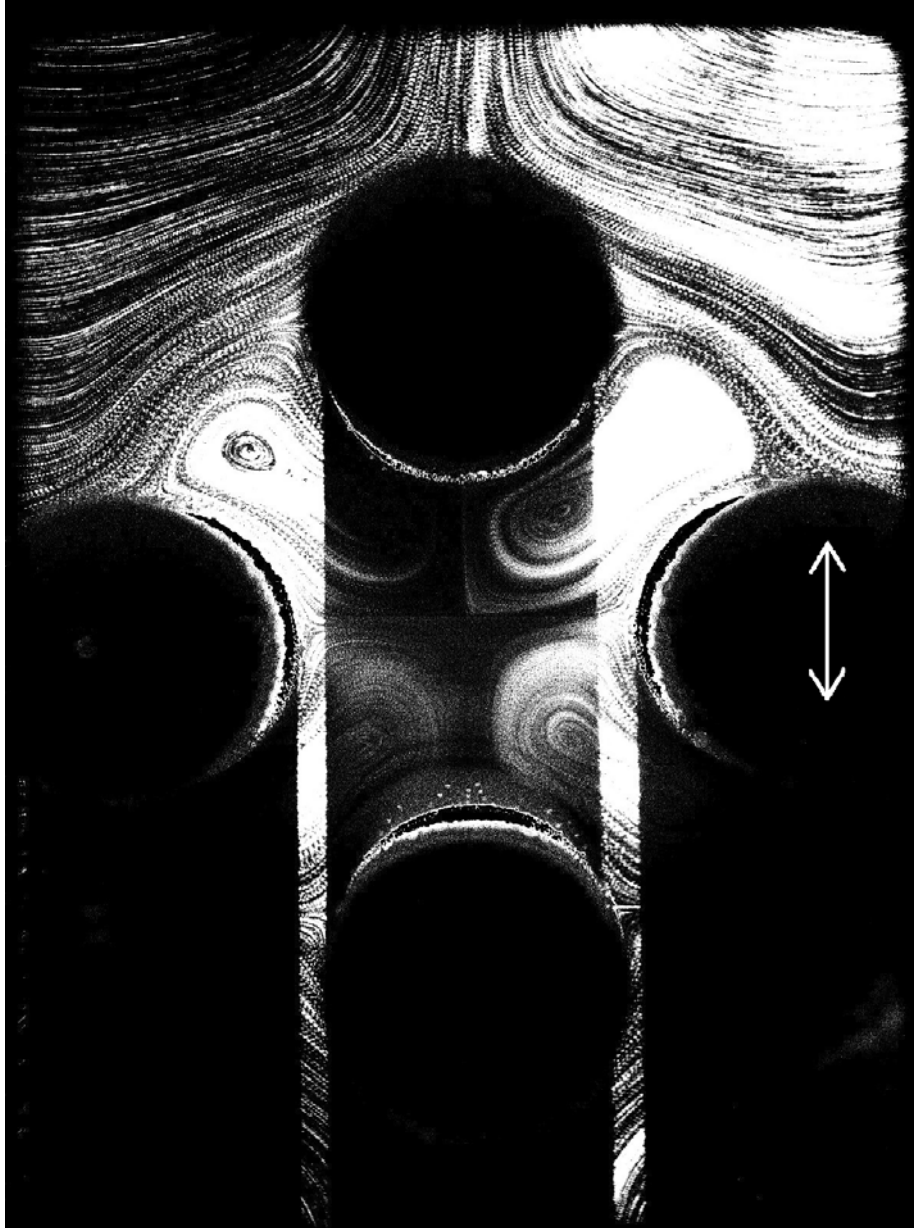


Figure 51: Streamlines distribution. Experiment B2:  $\varepsilon = 0.14$  y  $Rs = 168.74$

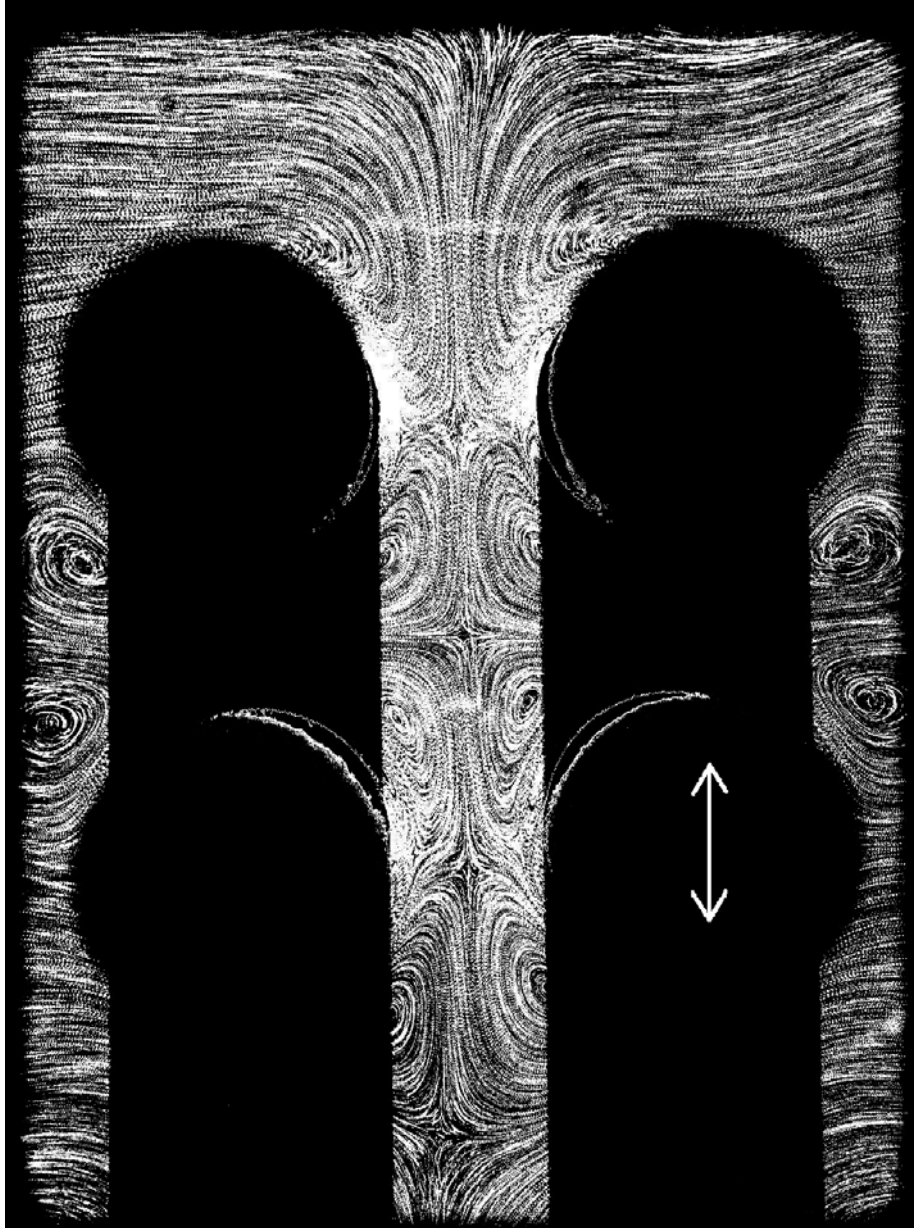


Figure 52: Streamlines distribution. Experiment C1:  $\varepsilon = 0.14$  y  $Rs = 73.70$



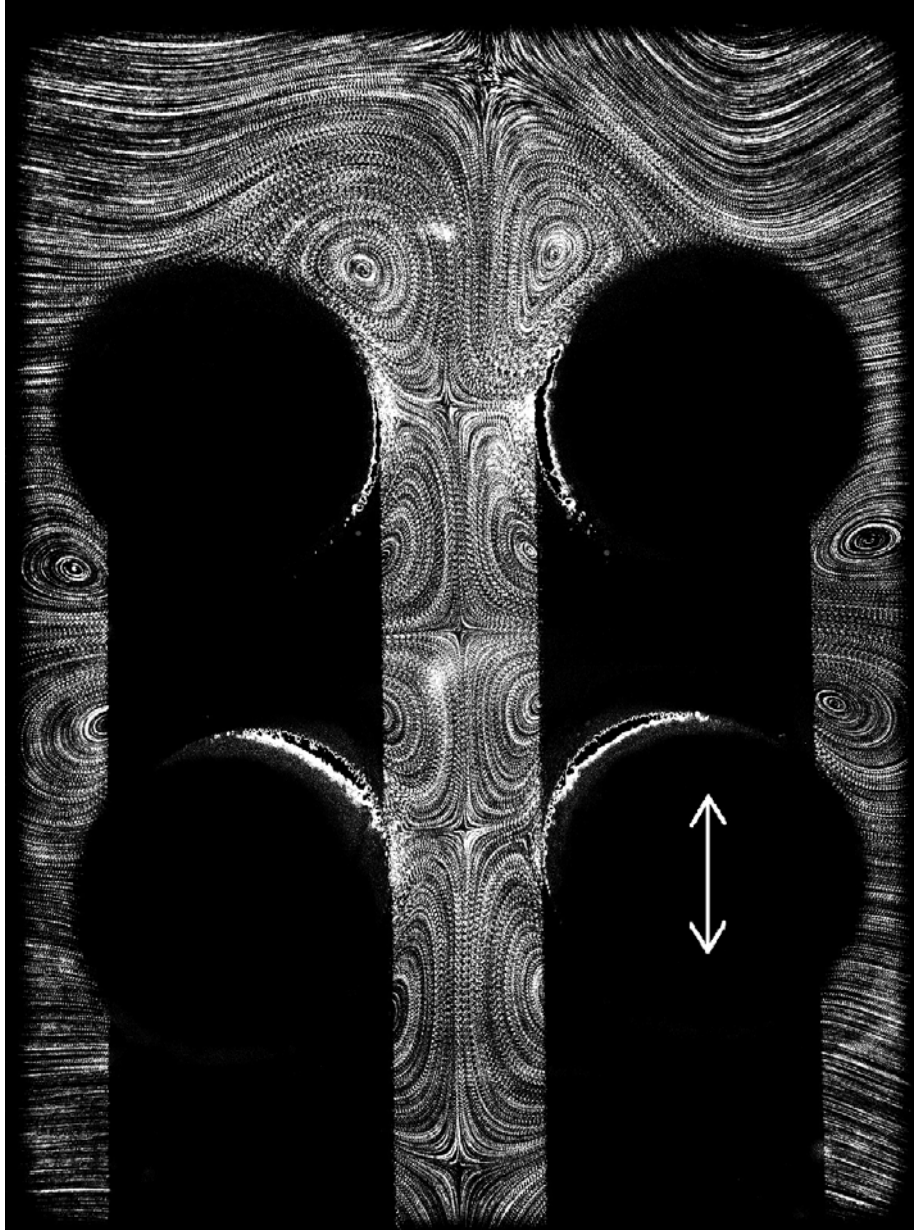


Figure 53: Streamlines distribution. Experiment C2:  $\varepsilon = 0.14$  y  $Rs = 167.77$



## • CONCLUSIONS •

## 5 Conclusions

### 5.1 Two cylinders

In the case of the experiments type A, the focus was on how the frequency of the movement suffered by the cylinders affects the generation of steady streaming. For this purpose, the velocity was raised during the experiments A1 to A4. As it has been explained, this modifies directly the key parameter  $Rs$ , and one of the aims of this research is to prove its importance for a potential ability to trap particles. Paying attention to the results coming from the experiments, some interesting conclusions can be obtained.

Firstly, it is interesting to confirm the results expected from the numerical analysis and the former researches about this case. Using run A4 as a reference, the appearance of all the main features of the steady streaming flow can be ratified. As it is displayed in the Figure 54, the existence of two main stagnation points SP1 and SP2 is viewable, as well as another in every side of the cylinder, S1. In these particular points, due to the movement of the bodies several flow currents meet at the same location carrying different directions, so they produce points where the fluid has zero velocity. In addition, the fluid is being ejected from the top of the cylinder at the point E1.

But what it is important to mention is the presence of another stagnation point at the centre of the recirculating cell which is actually why this phenomenon is interesting for trapping particles. Following the streamline drawn in the image, it can be confirmed that when a particle enters into the influence area of the steady streaming, can eventually end up in the centre of the vortex, which would be able to control its position. Studying what kind of particles can be influenced by this, depending on their size or density, shows up as the next natural step for this research and it could lead to real uses of the steady streaming for practical cases.

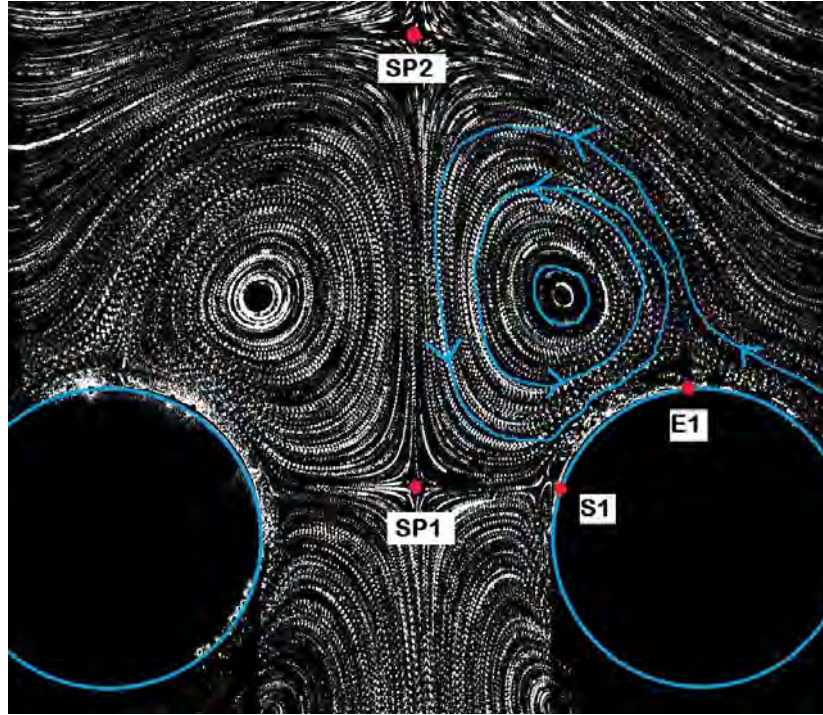


Figure 54: Detail of Experiment A4:  $\varepsilon = 0.14$  y  $Rs = 195.89$

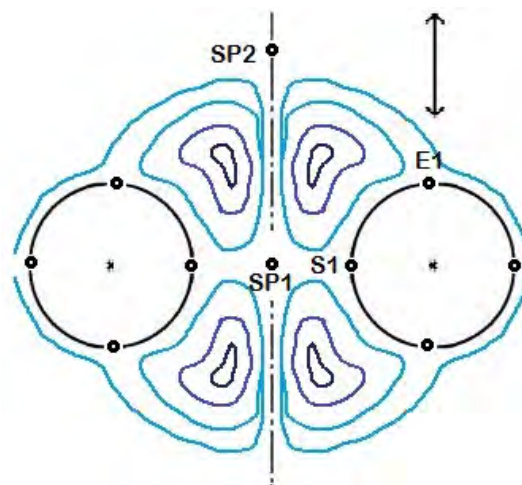


Figure 55: Diagram of steady streaming over two cylinders

However, comparing the images between experiments, it is easy to recognise that as the streaming Reynolds number increases, the steady streaming phenomenon can be identified more easily. The stability of the flow structures in experiments with relatively low frequency, like the run A1, is much weaker. This means that it is hard to achieve a symmetric structure and the stagnation point SP1 between vortices is often shifted randomly. Moreover, the recirculating cells are not strong enough to generate a whole circular vortex and as it is seen in Figure 54, the structure is open in one of its side. This would deeply affect the trapping capabilities of the device, making it difficult to maintain a particle in a fixed position.

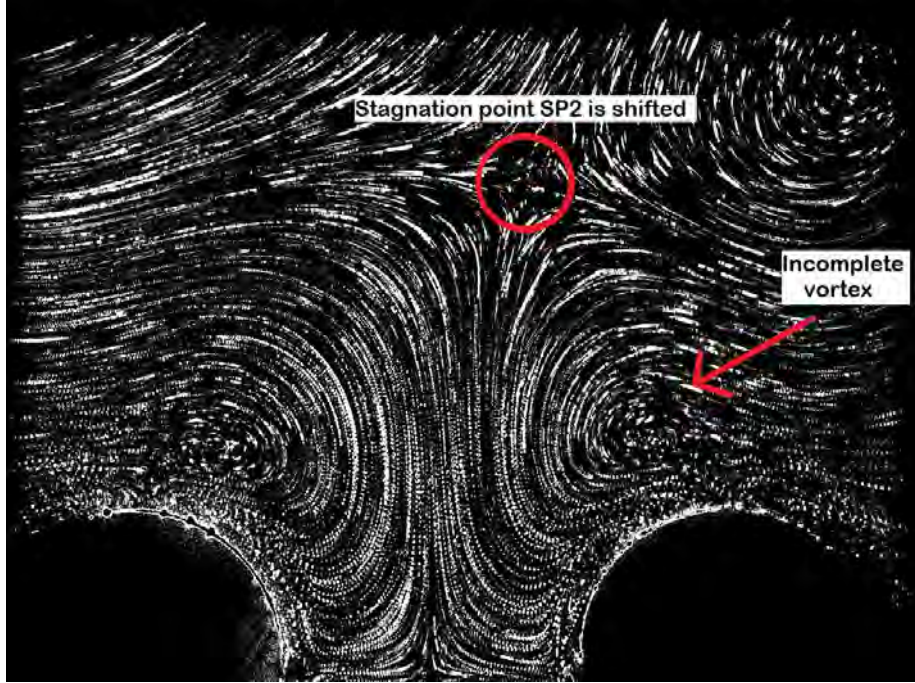


Figure 56: Detail of the streamlines for experiment A1.  $\varepsilon = 0.14$  y  $Rs = 71.76$

Nonetheless, as the  $Rs$  becomes higher, the flow pattern turns more stable and constrained, as well as it gains more symmetry. Paying attention to experiments A2 and A3 it can be affirmed that the vortices begin to get fully formed when  $Rs$  is between 100 and 140. After that, the centre of the recirculating cells start to change into almost circular paths, as in Figure 54. This means some

particles can be forced into these currents and get trapped.

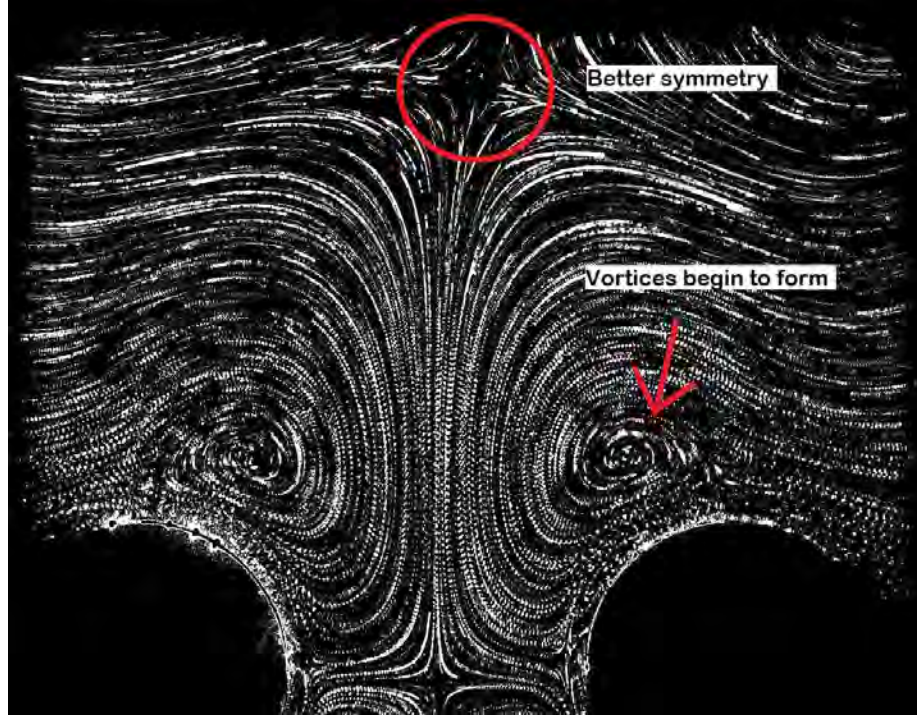


Figure 57: Detail of the streamlines for experiment A2.  $\varepsilon = 0.14$  y  $Rs = 97.94$

So it can be concluded that the experiments supports the previous hypothesis of the necessity of a high Reynolds number to use Steady streaming as a viable method of particle trapping.

By extrapolating these results, it can be said that for a non-dimensional oscillation amplitude of 0.14, the steady streaming seems suitable for controlling particles for  $Rs$  higher than 140. Nevertheless it would be interesting, as a continuation to this project, to study the real strength of the vortices and find experimentally the key parameters that define which particles can be trapped and which cannot.



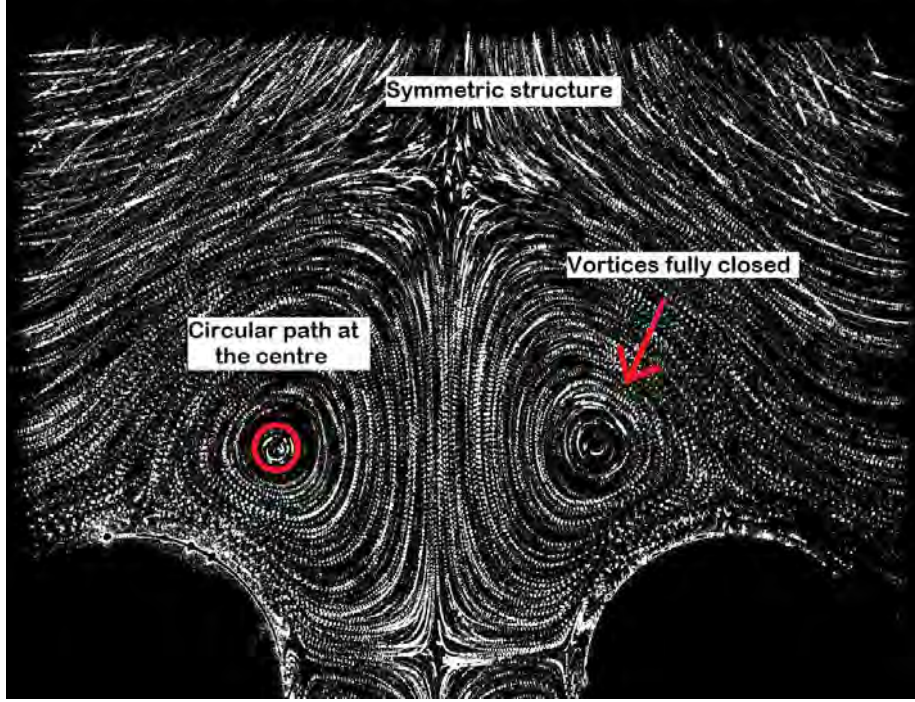


Figure 58: Detail of the streamlines for experiment A3.  $\varepsilon = 0.14$  y  $Rs = 144.49$

## 5.2 Four cylinders

In the case of using four cylinders, the aim of this project was to identify and analyse the flow patterns that this distribution produces. As it has been said, there are not former studies for this distribution and range of parameters. Only studies like House *et al.* (2014) which used an array of micro-cylinders could give a clue about how the fluid would response to the presence of more moving bodies.

As a first glance, importance differences can be noticed between experiments B and C. As it has been said, type B had the cylinders placed forming a diamond with respect to the movement direction. In the other hand, C was turned 45 degrees to form a regular square. This led to completely different results, although both are rather interesting for the purpose of this project.

Starting from experiments B1 and B2, it is noticeable that the former single vortices that appeared with a two cylinder distribution now changed into double vortices. However, they seem to maintain the same internal characteristic

of owning a stagnation point in each of their centres. This could lead to think that using this arrangement of solid bodies it is still a viable option for particle trapping purposes.

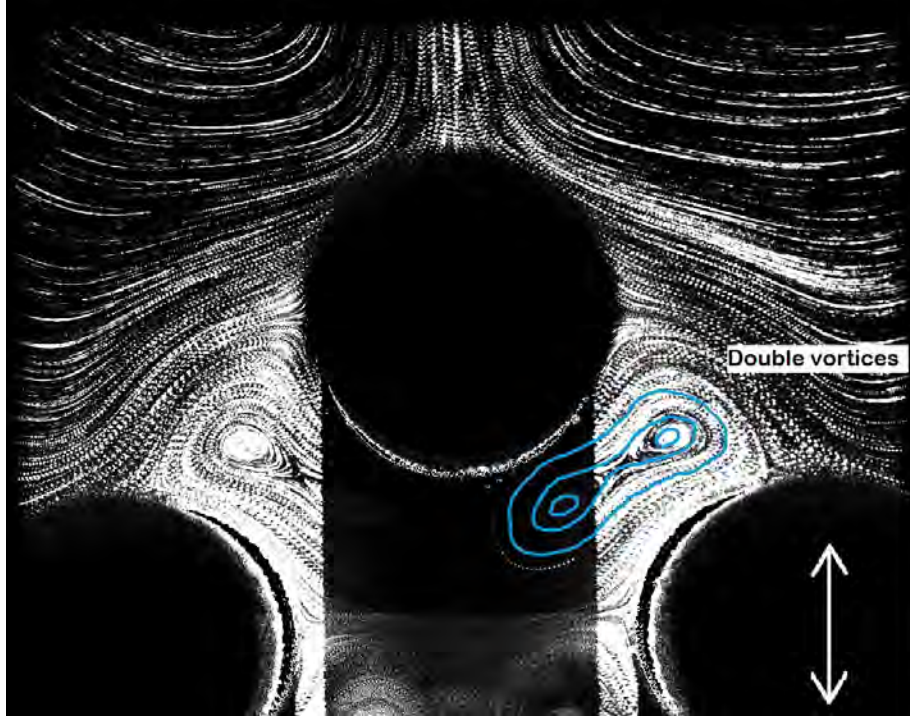


Figure 59: Detail of the streamlines for experiment B1.  $\varepsilon = 0.14$  y  $Rs = 168.74$

Moreover, the fluid is in this case less altered in the areas outside the cylinders. Meanwhile, the inner zone where the recirculating cells appear looks highly constrained by the bodies and quite stable.

Regarding, experiments type C, absolutely different results were obtained from the experiments. Despite what could be previously thought, the outcome include some similarities to the one using a two cylinders distribution.

One of the aspects that can be extracted that emerges as really interesting for this project is the fact that even for a small streaming Reynolds number, the four cylinders are able to generate quite stable vortices in the area between them. As it is seen in the experiment C1, which had a  $Rs = 73.70$ , the recir-

culating cells that are created in the surroundings of the bodies look unstable and not fully formed, as it also happened for experiments A1 and A2 with low  $Rs$  too. However, the vortices in the inner part seem to be stable enough to be used for particle trapping, probably due to the extra constraint of the new bodies.

Anyway, comparing experiments C1 and C2 it can be assured that for bigger streaming Reynolds numbers, the steady streaming phenomenon gains strength and stability.

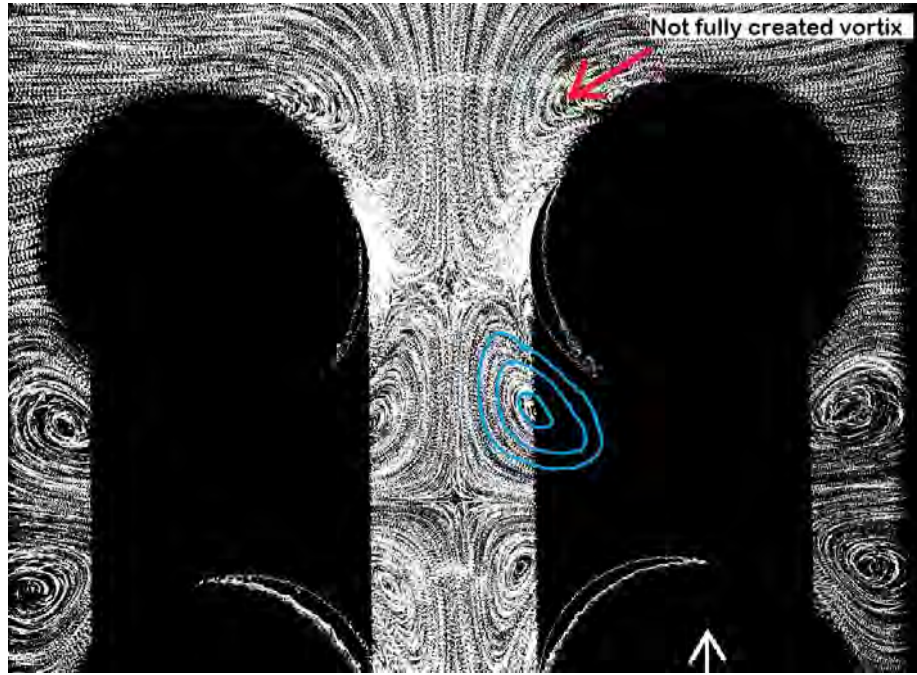


Figure 60: Detail of the streamlines for experiment C1.  $\varepsilon = 0.14$  y  $Rs = 73.70$

To conclude, it can be said that the results of this project endorsed the theoretical studies that encouraged the fulfilment of this research. The importance of the non-dimensional number  $Rs$  for creating a stable steady streaming has been proved, as well as a small non-dimensional oscillation amplitude  $\varepsilon$ . Furthermore, it was possible to provide a specific range of values for  $Rs$  where the steady streaming begins to be considered fully developed (between 100 and 140) for  $\varepsilon = 0.14$ .



## • BIBLIOGRAPHY •

# Bibliography

- AMET, F. 2009 Cooling and trapping techniques with ultracold atoms. *Physics* **376**, Stanford University .
- AN, H., CHENG, L. & ZHAO, M. 2011 Direct numerical simulation of oscillatory flow around a circular cylinder at low keulegan-carpenter number. *J Fluid Mech* **666**, 77–103.
- COENEN, W. & RILEY, N. 2009 Oscillatory flow about a cylinder pair. *Q J Mech Appl Math* **62** (1), 53–66.
- DAVIDSON, B. J. & RILEY, N. 1972 Jets induced by oscillatory motion. *J Fluid Mech* **53** (2), 287–303.
- DING, X., LIN, S. S., KIRALY, B., YUE, H., LI, S., BENKOVIC, S.J. & HUANG, T.J. 2012 On-chip manipulation of single microparticles, cells and organisms using surface acoustic waves .
- GALAN, E. 2013 Estudio experimental y numerico del flujo oscilatorio alrededor de dos cilindros .
- HOUSE, T. A., LIEU, V. H. & SCHWARTZ, D. T. 2014 A model for inertial particle trapping locations in hydrodynamic tweezer arrays. *J Micromech Microeng* **24**, 045019.
- KOTAS, C. W., YODA, M. & ROGERS, P. H. 2007 Visualization of steady streaming near oscillating spheroids. *Exp Fluids* **42**, 111–121.
- RILEY, N. & WYBROW, M. F. 1995 The flow induced by the torsional oscillations of an elliptic cylinder. *J Fluid Mech* **290**, 279–298.
- SADHAL, S.S. 2012 Acoustofluidics 13: Analysis of acoustic streaming by perturbation methods. *Lab on a Chip* .

VOLDMAN, J., GRAY, M.L., TONER, M & SCHMIDT, M.A. 2002 A microfabrication-based dynamic array cytometer .

WYBROW, M. F., YAN, B. & RILEY, N. 1996 Oscillatory flow over a circular cylinder close to a plane boundary. *Fluid Dyn Res* **18** (5), 269–288.